SSEC No.71.08.M1

Dept. of Meteorology
University of Wisconsin

A SATELLITE STUDY OF CLOUD CLUSTERS OVER THE TROPICAL NORTH ATLANTIC OCEAN

David W. Martin

V. E. Suomi

Space Science and Engineering Center

The University of Wisconsin

Madison

Final Report on Tropical Cloud Organization Studies,

Task Order Number 3 to STAG Contract E-127-69-(N)

13 August 1971

Reading Room
Dept. of Meteorology
University of Wisconsin

Reading Room
Dept. of Meteorology
University of Wisconsin

ACKNOWLEDGEMENTS

Of the many people who had a hand in this report, the following persons made an especially noteworthy contribution: David E. Cadle and Jerome Lawler, Photography; John T. Young, precision display; Michael Garber, Debby Berndt, Michael McCaskill and Geoff Legler, analysis; Vicki R. Epps and Linda L. Martin, typing. Michael D. Hudlow and Wolfgang D. Scherer of the BOMAP Office kindly supplied radar images and assisted in their interpretation.

Reading Room
Dept. of Meteorology
University of Wisconsin

SUMMARY

The focus of this study is cloud clusters over the tropical Atlantic Ocean. Census and case study analyses have shown that

- the eastern Atlantic is at least as convectively active as the western Atlantic during June and July, and has a significantly greater total area of cloud clusters.
- convective cores have a great range of size, spacing, and lifetime; nevertheless an ordering invariably can be perceived. This most often is as lines or bands; waves, spirals, or solitary cores are are also observed. Lifetimes are a few minutes to several hours or more; large cores last longer.
- displacement of cloud clusters is accomplished by a complex combination of band and cell movement and propagation. Structure, as evidenced by core behavior, is varied and complex.

The method of analysis, being unconventional, received an inordinate amount of attention. Review of the ATS signal processing system revealed a number of flaws, some of which are under SSEC control, some of which are not. Those beyond our effective control include highly variable satellite and ground station gain settings, one of which for over a year was totally undocumented, gain settings which produce saturation in active clusters close to the solar subpoint and slight clipping of a nominal 10 volt signal at the ground station. Others which to a large extent have been rectified are the setting of the NRZ and zero levels and uniform photographic processing of enhanced pictures. These problems were troublesome, but not insurmountable. Their chief effect was to limit the mass of data suitable for analyses of the kind undertaken.

Through improvements in signal processing and circumvention of unsolvable problems by judicious data selection, it has been shown that in spite of all difficulties signal enhancement is an effective, precise tool for isolating selected features of ATS images. Comparisons of ATS and radar images have established the high correlation of bright areas on ATS with large radar echos; therefore, enhanced ATS pictures emphasizing the upper levels of the brightness range effectively isolate deep convection. The brightness structure of convective clouds is such that they can be studied over a three to four hour period around local noon on pictures uncorrected for changes of incident and reflected radiation. A simple cosine law correction for incident radiation can appreciably extend this period.

I. Introduction

To assist the GARP Study Group on Tropical Disturbances at its first meeting in 1968, meteorologists of the Space Science and Engineering Center made a census of cloud systems over the tropical Pacific Ocean (Martin and Karst, 1969). Following the recommendation of the Brussels Planning Conference on GARP (1970) that the location of the Tropical Experiment be changed from the Pacific to the Atlantic Ocean, it was proposed early in 1970 that a similar census be made by SSEC for the Atlantic. The immediate purpose of this census was to provide a sounder basis for deciding whether to conduct the Experiment in the eastern or western Atlantic. Through a technique of ATS signal enhancement the study would in addition give insights on convective activity within cloud clusters.

Developments since then have in some ways altered the emphasis of the investigation. The decision in favor of the eastern Atlantic (Report of the Fifth Session of the JOC, 1971) advanced convective studies to first priority. Comparisons of satellite and radar images are aimed particularly at answering a need expressed in the revised Plan for U. S. Participation in the GARP Atlantic Tropical Experiment (1971), that the observational plan "...will rely on radar and satellite data for determining the position, size, shape, and intensity of the mesoscale convective systems within the network." Detailed case studies contribute to the scientific and logistic planning of the Experiment by depicting the configuration, internal structure, and evolution of convective systems, and by revealing differences between east Atlantic and other cloud clusters.

Some of these results have already contributed to the planning of GATE. Parts of the census on cloud clusters were introduced at the 1971 Bombay meeting of the Joint Organizing Committee (Report of the Fifth Session of the JOC, 1971); enhance-

ment as a technique for isolating convection was discussed at the Geneva meeting on the use of aircraft (Report of the Informal Planning Meeting on the Use of Aircraft in GATE, 1971).

This report presents the results of the Atlantic census and analysis of convection using the enhancement technique. Because these results depend so critically upon the interpretation of ATS data, they are prefaced by a discussion of the ATS signal processing system. The reader is warned against being intimidated by the complexity of this discussion. The reward for perservering is a solid understanding of the limitations and the potential - some of which is demonstrated in later sections - of data from the ATS Spin Scan Camera System.

II. ATS Signal Processing

Hardware

The need for a uniform, reproduceable data product of known characteristics has prompted a complete review of the ATS III data processing system. Although the review to date has focussed on elements related to the measurement of cloud displacements (Parent, 1971), the picture production system has also come under scrutiny.

Signal flow

ATS III data flow is depicted in Figure 1. Part (a) covers the system from spacecraft through ground station. Points of particular concern to meteorological use of the signal are camera and ground station gain settings and NRZ (Non-Return Zero) level setting. Camera gain setting is ground commanded to any of four step positions. Ground station gain is set at the attenuator to any of six levels which are in 2-db increments. These gain settings are automatically encoded within the NRZ. At nominal settings for camera and ground station gains bright clouds close to the satellite and solar subpoint will, by design, just saturate the camera photometer (Technical Data Report for ATS, 1968).

Within the NRZ is a reference signal which has a fixed (2/3) relation to the voltage range handled by the system. This NRZ reference is added to the data signal at the color video processor in the ground station, after gain adjustments have been made. It is not adjustable.

Proper setting of the NRZ is a critical step in the production of pictures and digital tapes from analog tapes (Figure 1b). Over the past year this operation has been refined from eyeballing an oscilloscope ($\pm$ 5 % accuracy) to digital readout of the NRZ voltage ($\pm$ 0.5 % accuracy).

To fix the signal amplitude a zero reference in the NRZ is adjusted to zero voltage. The accuracy of this operation has been improved to about $\pm$ 0.5 % by the recent installation of a zero level electronic clamp.

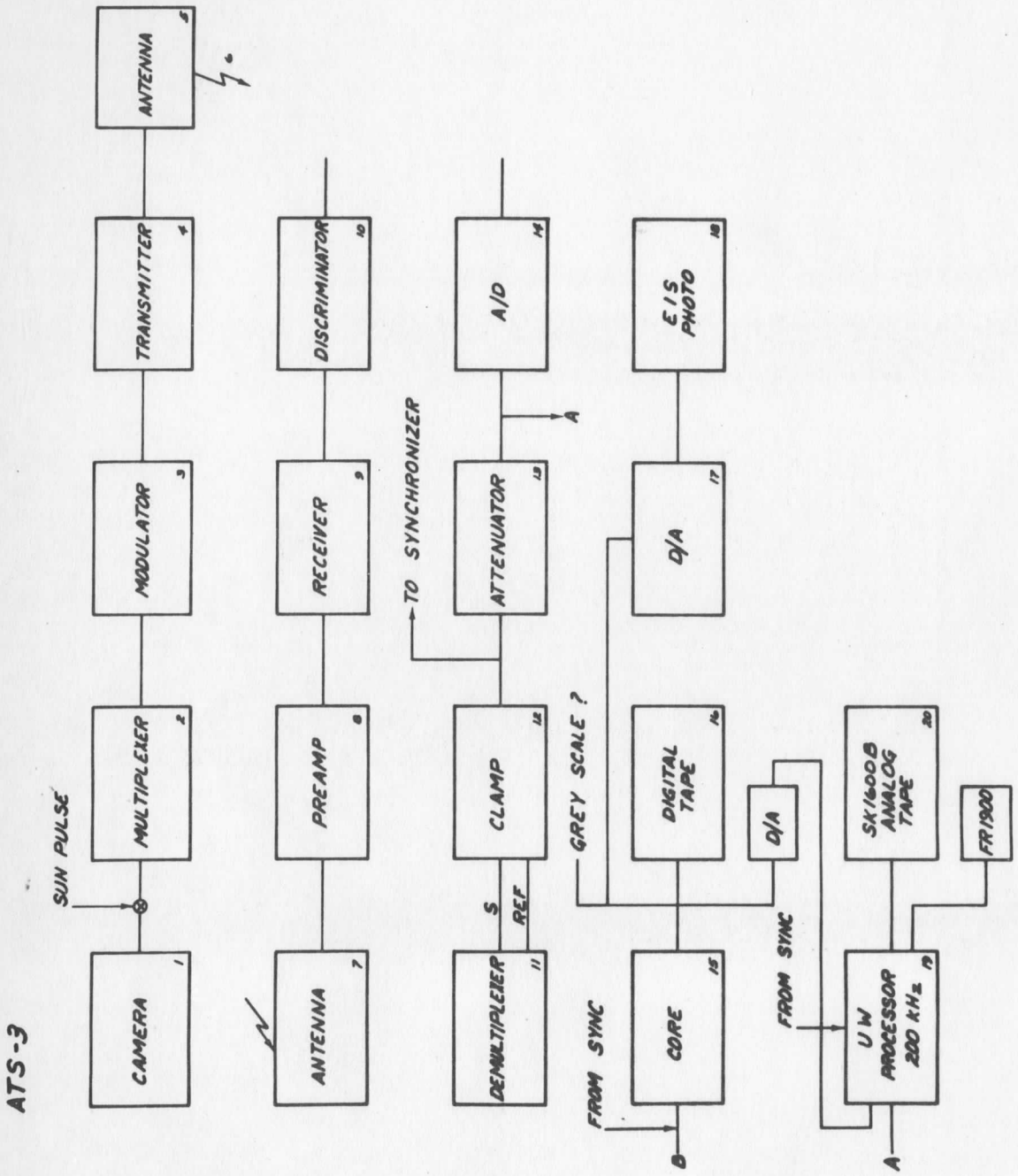

Figure 1.a Data flow through the signal processing system for ATS III - Spin Scan Camera and ground station.

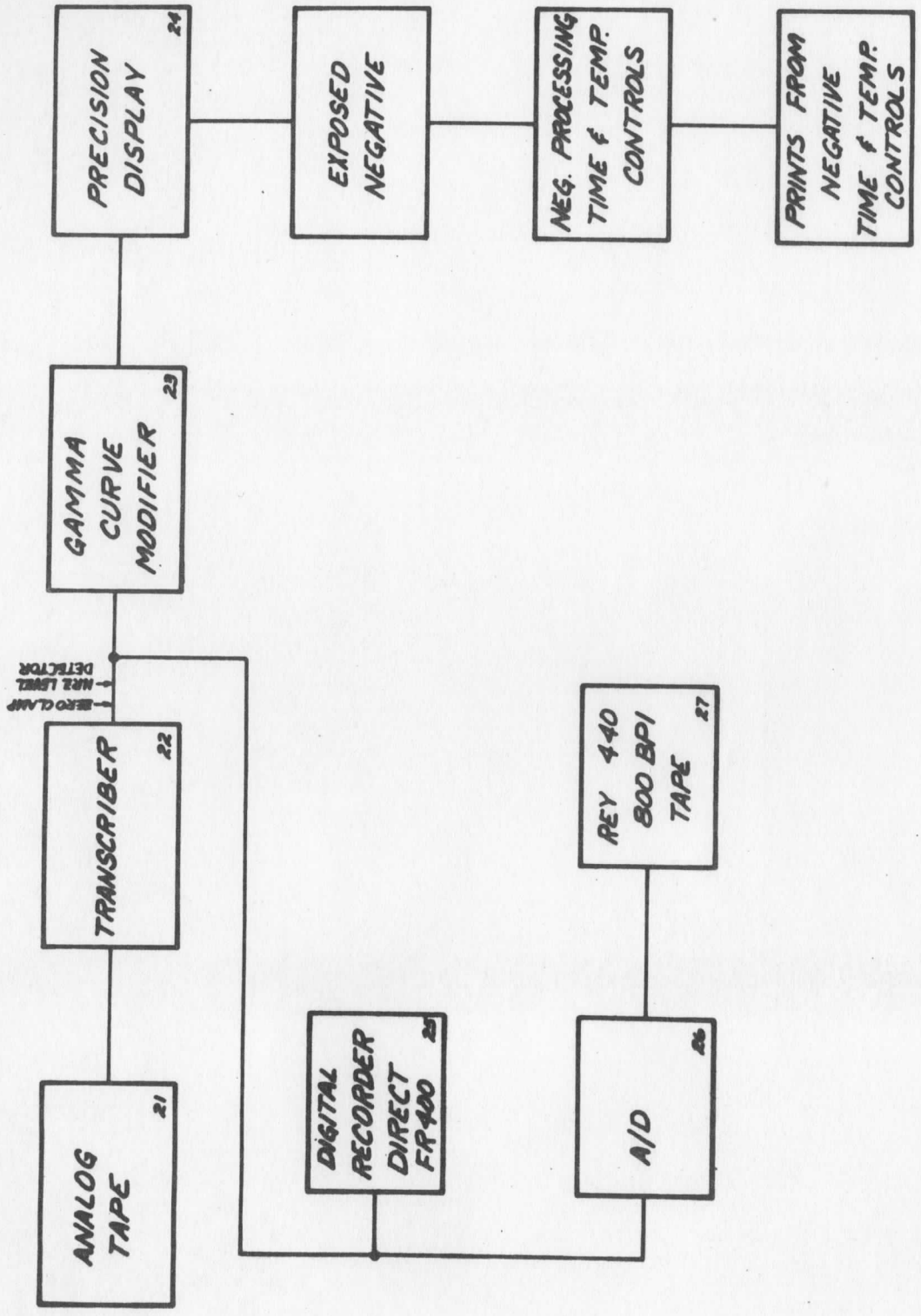

Figure 1.b Data flow through the signal processing system for ATS III - processing of taped signals within SSEC.

Limitations

A problem not amenable to control through special electronics is saturation of the signal in active cloud clusters near the satellite subpoint. Line plots through clusters and frequency distributions of digital radiance for clusters (Figure 2) show that limited saturation occured at the 3, 10 camera and ground station gain settings typical for the last seven weeks of BOMEX.

This saturation is a part of system design and can be removed through gain adjustment. It is distinct from clipping, which occurs at some voltage lower than the nominal 10 volts the system is designed to handle. Measurements of saturation voltage using the NRZ level detector and zero level clamp to fix signal references showed saturation occurring at 9.50 to 9.72 volts; that is, a 3 to 5% reduction in the nominal 10 volt signal range. This clipping originates at the ground station. It is limited to areas close to the solar subpoint and therefore, for present uses of the data is considered to be inconsequential.

Ground station gain settings

After movement of the ATS ground station from Rosman, North Carolina to Wallops Island, Virginia ground station gains were varied to preserve a maximum amplitude of the data signal (Gage, 1971). Unfortunately gain adjustments were made in the video amplifier and, therefore, were not recorded in the NRZ. Since no documentation was made, the actual gain settings are lost, unless they can be recovered from the data.

An effort was made to infer gains from densitometric measurements of a salt flat in South America, Salar de Uyuni (67° W, 20° S), using 24 days of archive negatives borrowed from the Environmental Satellite Center, Suitland, Maryland. Measurements were made on a MacBeth Quantalog transmission densitometer. Typical results are shown in Figure 3. The densitometer trace through the course of a day does show changes; however, attempts to relate these changes to overall changes in pictures from the precision display were unsatisfactory. Evidently variations in processing of the negatives and measurement errors of the densitometer as well as

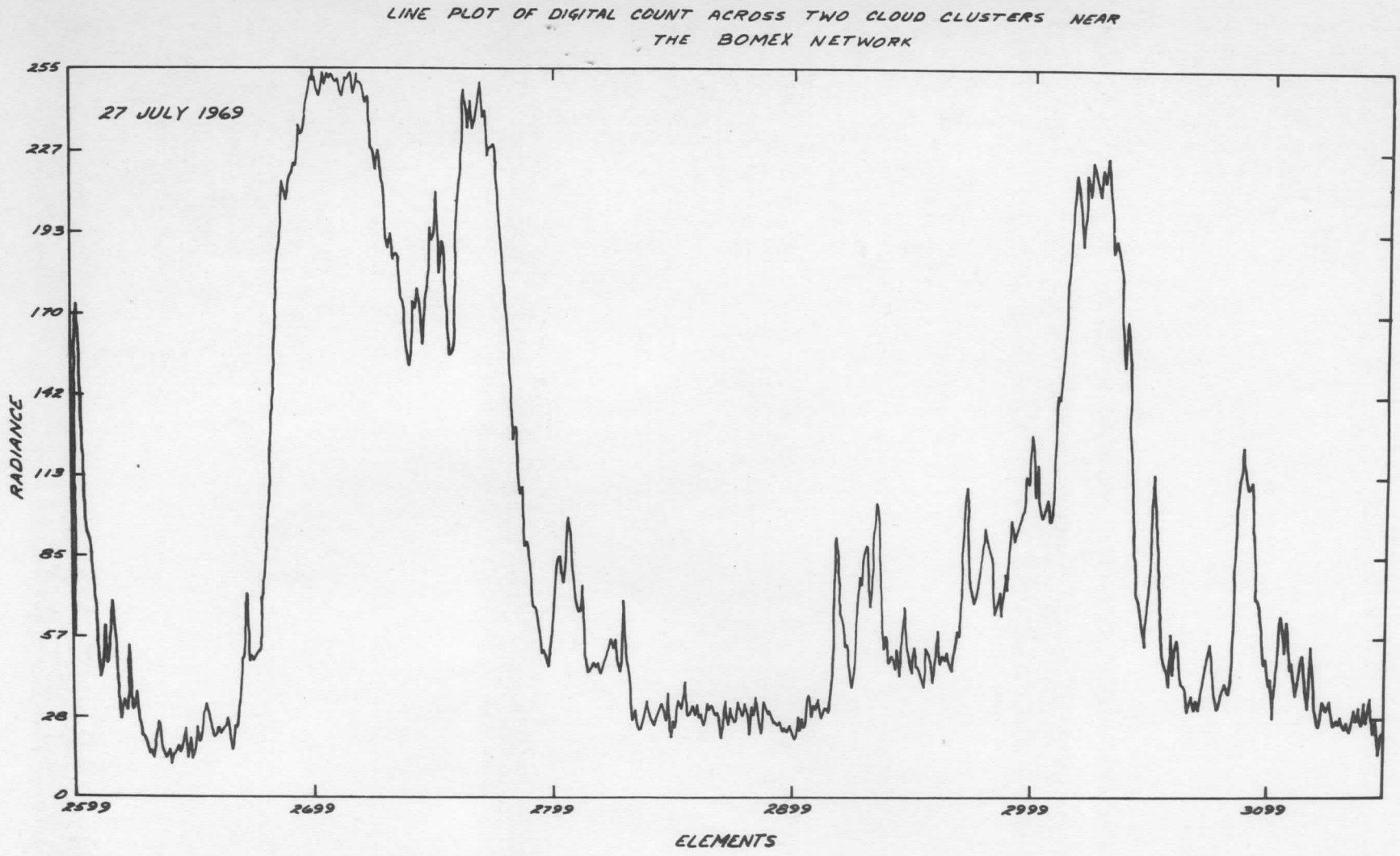

Figure 2. Profile of radiance across two cloud clusters east of Barbados; recorded by a single scan of the Spin Scan Camera.

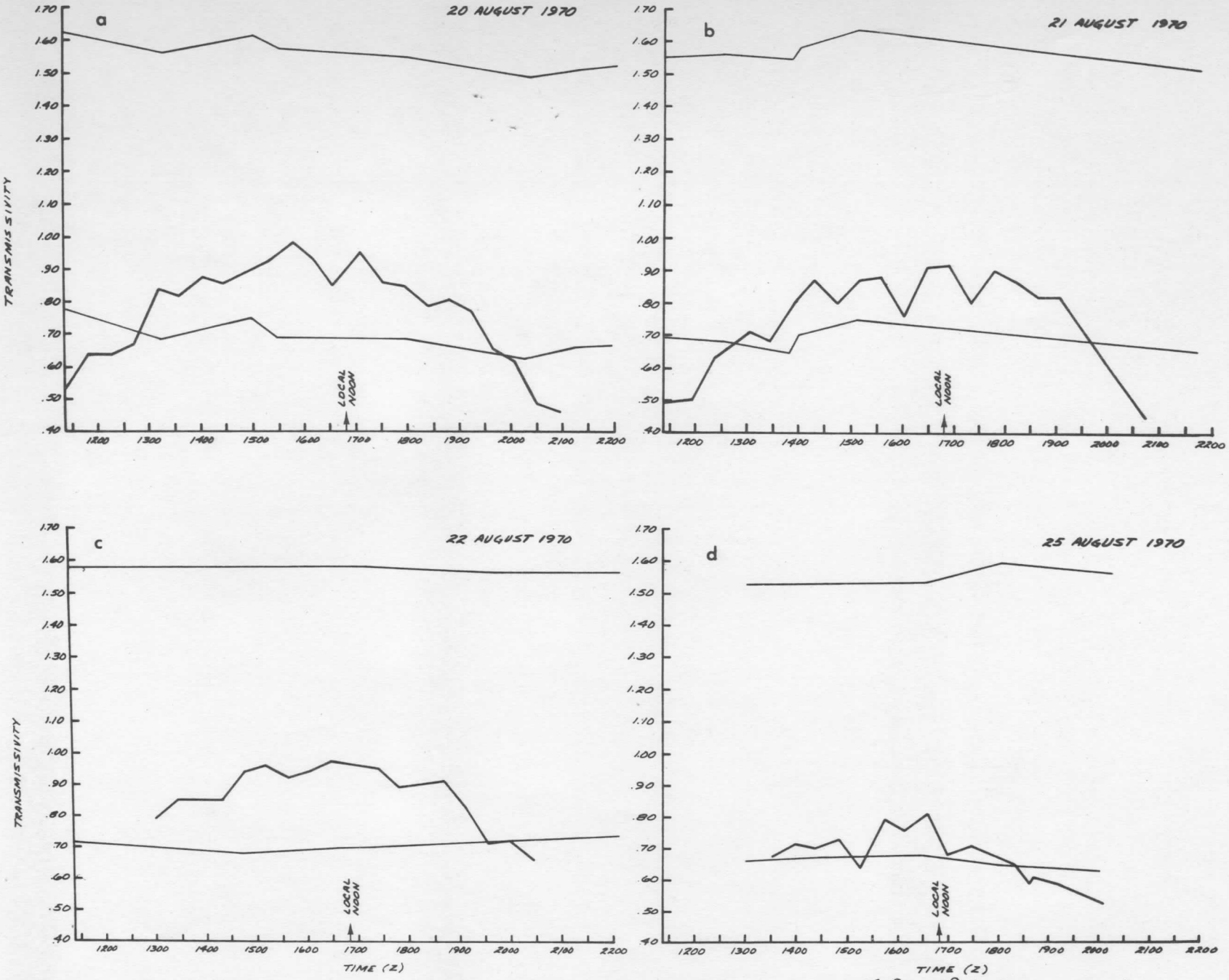

Figure 3. Densitometric measurements of the salt flat Salar de Uyuni (67°W 20°S) (heavy line) with sensitometer strips showing changes in negative processing (thin lines).

contamination of the salt flat by clouds are sufficient to mask all but the largest ground station gain changes.

Enhancement

Theory

Enhancement is an operation which emphasize selected portions of the linear curve relating radiance to signal strength. It can be accomplished digitally on a computer or by electronic (analog) devices. The computer offers great versatility, but cannot match the enhancement box for simplicity, efficiency, and cheapness. Therefore, since this study required large numbers of pictures, all of the enhancements analyzed are products of an enhancement box. This box, which was designed and built at SSEC (Schwalenberg, 1971), has five controls for setting three slopes and two break points. The case 4 transfer function used for the present study is shown in Figure 4a.

Transfer functions for film and print paper are shown in Figure 4b and c. The resultant true transfer function incorporating enhancement box and all stages of photographic processing is given in Figure 4d.

Experience gained through picture production and use, and the insights provided by line plots and frequency distributions of radiance in cloud clusters have led to refined criteria for an optimum transfer function. This improved enhancement, for typical gain settings, isolates deep convective clouds from other clouds, distinguishes between the darker sea and vegetated land surface for easy navigation, and distinguishes between thin cloud and vegetated land (and therefore, sea except in areas of strong sun glitter) for cloud displacement determination and area comparisons of cores and clusters. In form it resembles the case 4 transfer function. Actual slopes and break points would depend on photo processing materials and techniques.

Limitations

The isolation of deep convective clouds by the enhancement technique depends

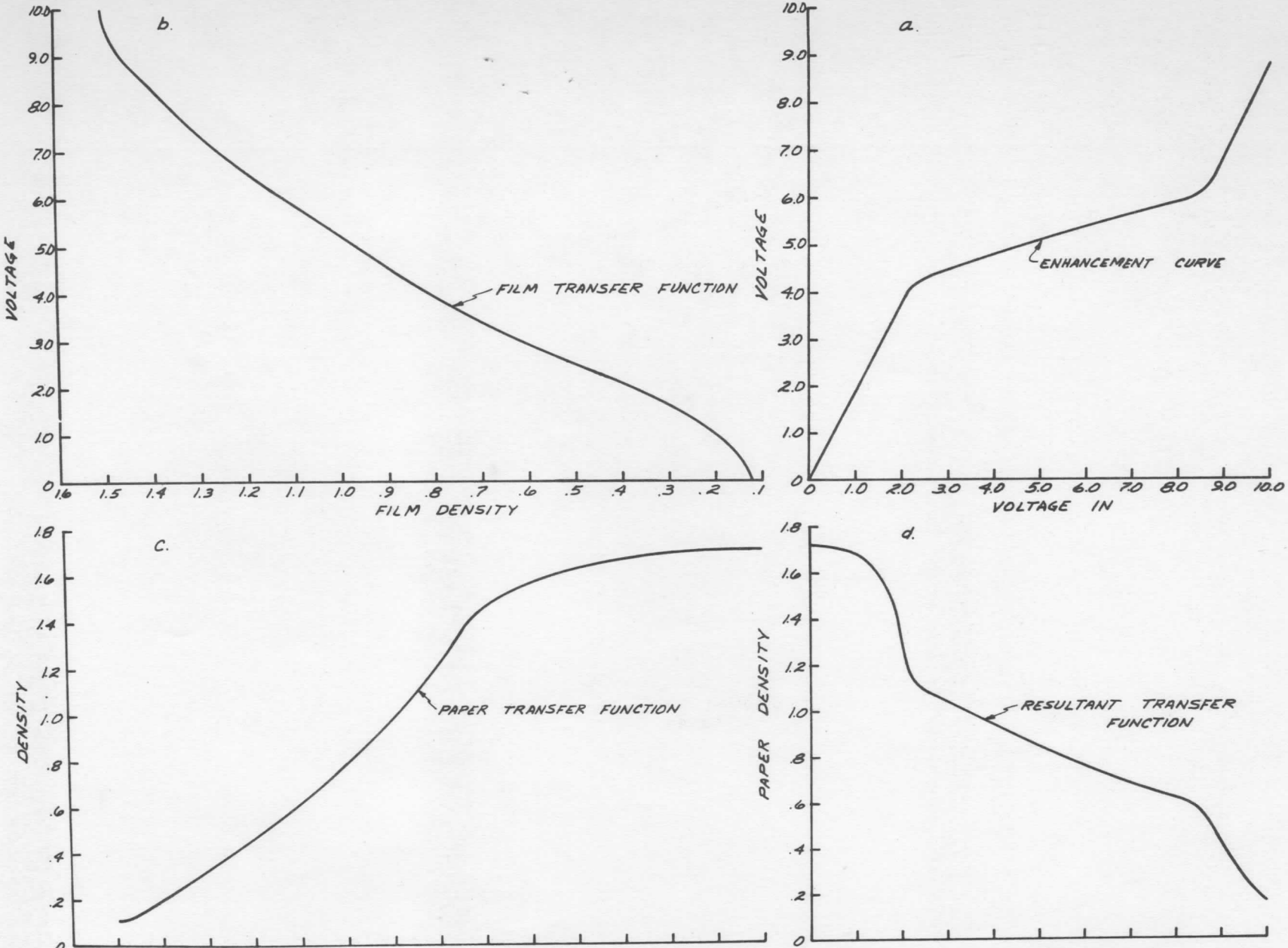

Figure 4. Transfer functions for enhanced pictures used in the present study. Part (a) case 4 enhancement curve; (b) film transfer function; (c) paper transfer function (d) resultant transfer function for the photos used.

upon these clouds having higher reflectance for a given geometry than other clouds. Assuming this to be so, the enhancement transfer function is set so as to markedly increase the difference in signal strength between levels corresponding to deep convective clouds and other clouds.

Saturation limits such discrimination by eliminating all detail above a certain level. In practice the problems connected with saturation were circumvented through selection of tapes having relatively low gains. The limited saturation occurring on these tapes removed details of structure in deep convective cloud tops, without significantly impairing the effectiveness of enhancement in isolating areas of deep convection. This is illustrated by line plots of radiance across a cloud cluster, which show flat or rounded peaks and steeply sloping sides (Figure 2). Limited saturation merely truncates the peaks. It is apparent from the signal transformations of Figure 5 that because of this profile structure inaccuracies in the setting of zero signal and NRZ levels affect contrasts between bright spots and other clouds much more than they affect spot areas. That the position of the radiance peak above or below the upper break point on the transfer function is critical to whether or not enhancement produces bright spots is clear from the lower part of Figure 5, where the range on the incoming signal has been reduced to 9 volts.

Radiation geometry has a profound effect on the satellite perceived brightness of a cloud and hence the enhanced picture of that cloud. If attenuation and scattering by the atmosphere are ignored, the radiation incident on a horizontal cloud is proportional to the cosine of the solar zenith angle. For a Lambertian surface the amount of radiation reflected is independent of the viewing (satellite zenith) or relative angles. Measurements show that clouds in general are not Lambertian reflectors (Ruff, et.al., 1967); however, because these measurements have not been made on cumulonimbus tops in isolation, the extent to which cb tops are non-Lambertian in their reflectance characteristics is not known. That they

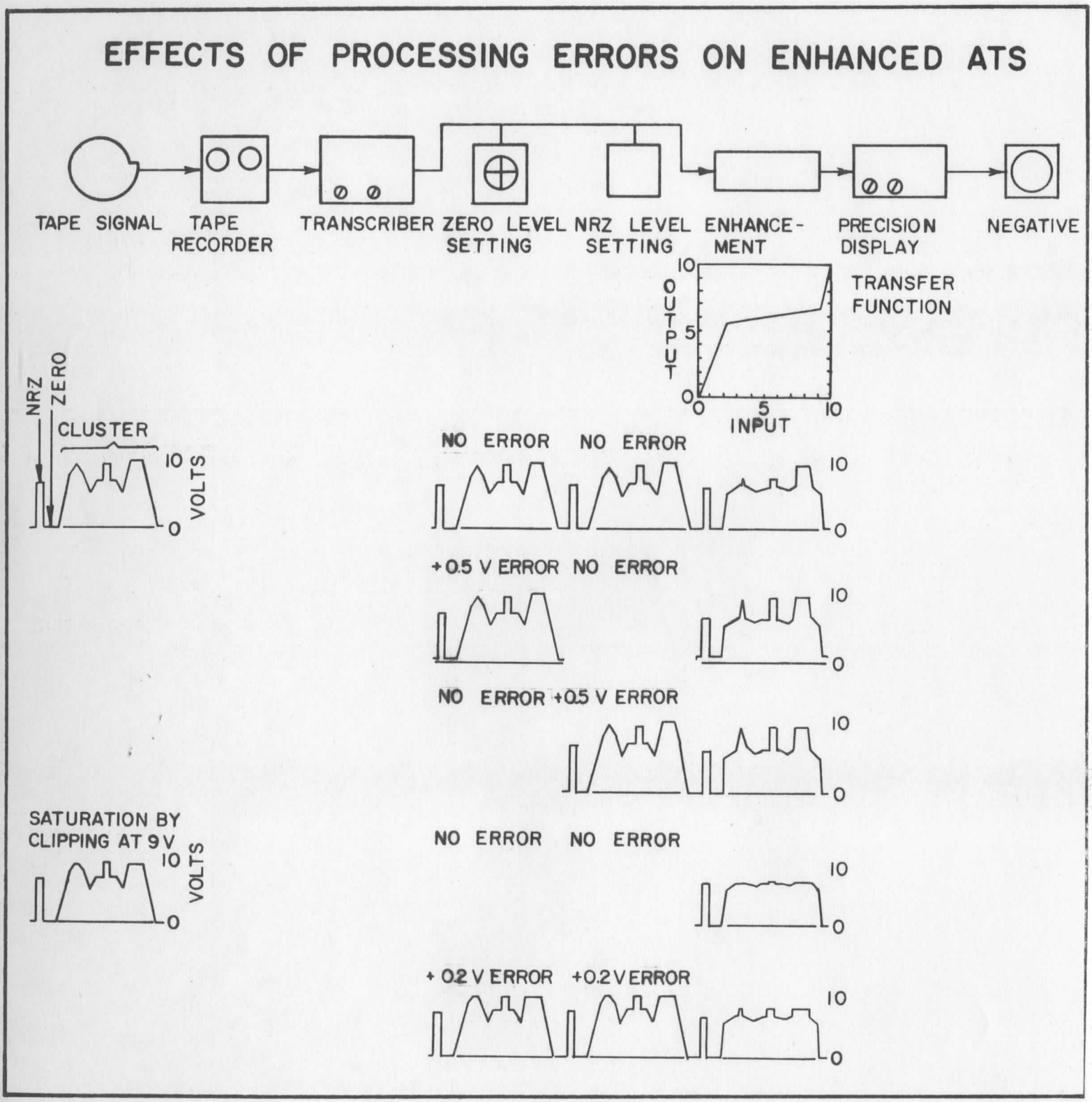

Figure 5. Schematic of the SSEC precision display system showing the effects of processing errors on a hypothetical signal containing NRZ level, zero level, and three types of cloud radiance profiles.

may be quasi-Lambertian is suggested by measurements of time changes in the longitude of the center of brightness on a complete day series of enhanced ATS pictures (Figure 6a and b). This center is the average longitude of the easternmost bright spot and the westernmost bright spot in a given picture. When the entire spot area is inside the eastern and western limbs of the earth the brightness center moves with the solar subpoint rather than, for example, the point of equiangular reflection between sun and satellite.

If at small solar zenith angles cb tops do behave as Lambertian reflectors, for the geometries prevailing in the pictures under consideration the cosine effect alone is of significance. The analysis which follows shows over what ranges of solar zenith angle it is practical to use a single enhancement for isolating deep convective cores.

In Table 1 the solar zenith angle is computed for increments of 14 minutes from local noon, at which time it is assumed the solar zenith angle is zero. By the cosine law these solar zenith angles are converted to radiance deficits for a Lambertian surface of constant albedo.

For times up to 70 minutes before and after local noon the total range of radiance due to changes in solar zenith angle is less than 5 %; for times up to 112 minutes before and after local noon it is less than 12 %. The effect of these changes on a model cloud is seen in the examples below.

We suppose that there exists a steady state, circular, deep convective cloud whose outer boundary (as might be determined by radar) coincides with the 210 digital count contour on an ATS picture taken at t = 0 (sun directly over the cloud center - see Figure 7). At some time $t \neq 0$ the 210 digital count contour will have shrunk so that it no longer coincides with the cloud boundary. The distance between contour and cloud boundary will depend on the brightness gradient across the cloud as well as the time difference from local noon.

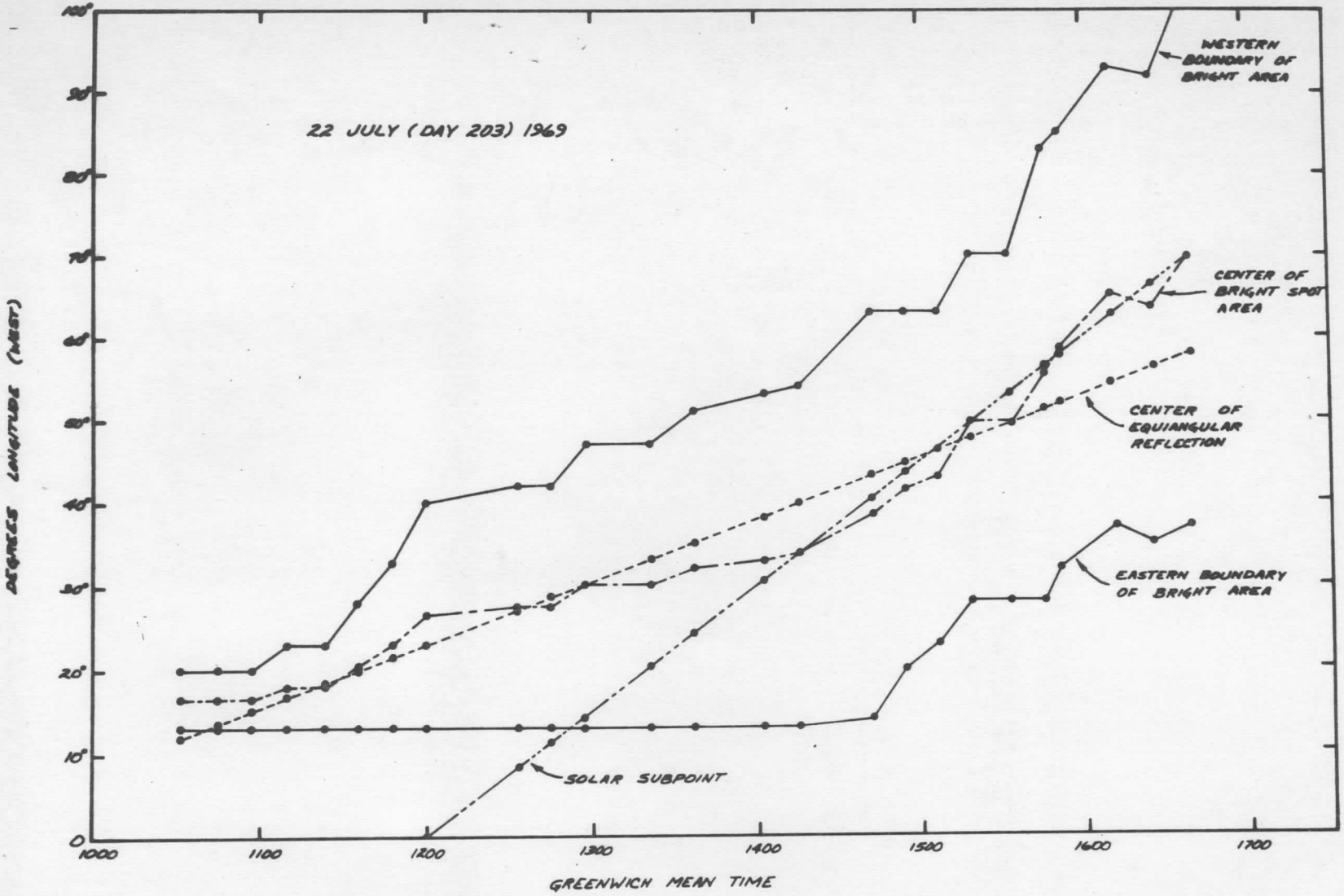

Figure 6.a Longitudinal change of the geometrical center of the bright spots on a complete day series of ATS pictures. Horizontal portions of either boundary represent extension of the bright spot region to the limb of the earth. 22 July 1969.

Figure 6.b As for Figure 6.a, except 22 August 1970.

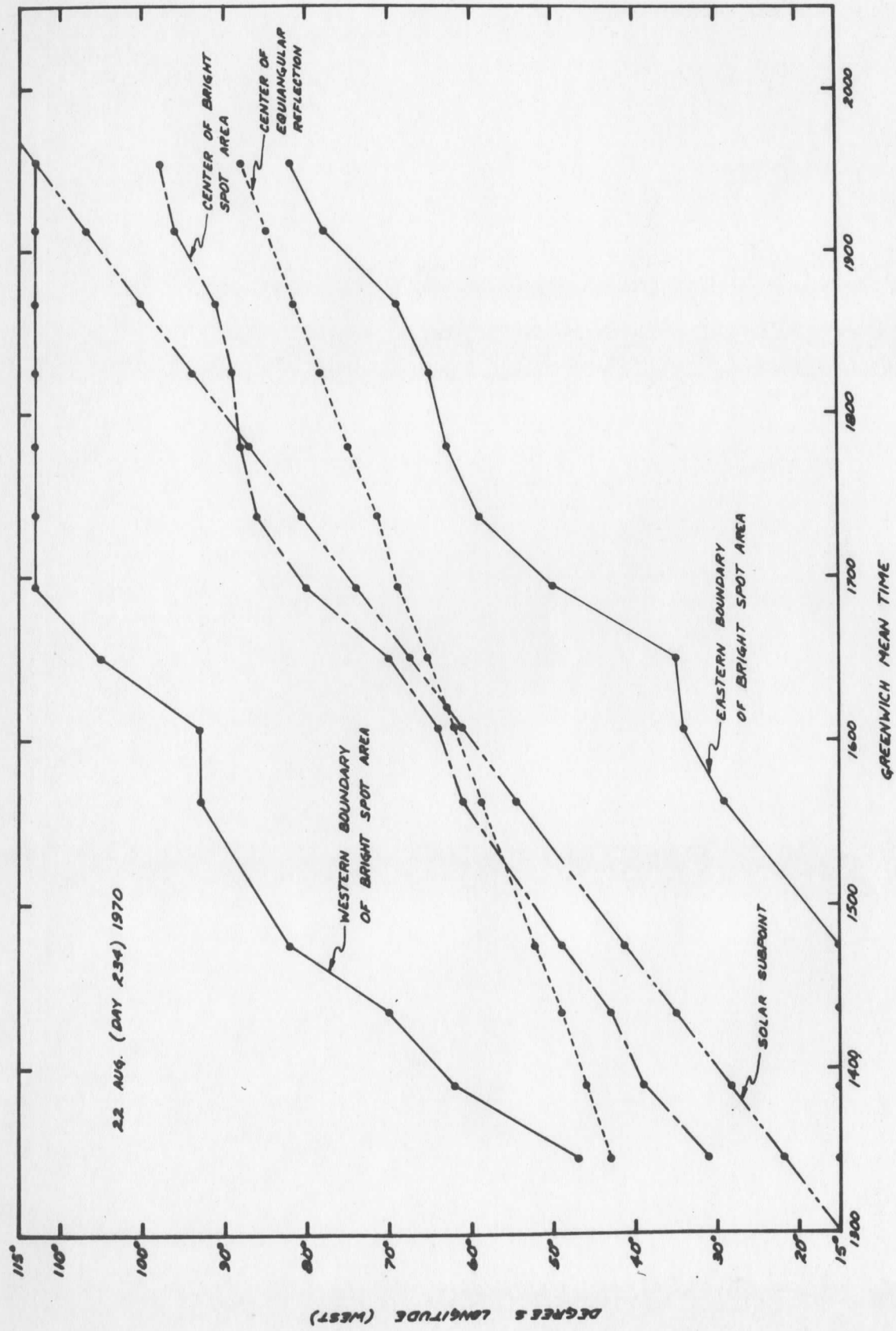

Table 1. RADIANCE CHANGES DUE TO INCREASING SOLAR ZENITH ANGLE

time t_i	0	14	28	42	56	70	84	98	112	minutes
solar zenith angle $_i$	0	3.5	7	10.5	14.0	17.5	21	24.5	28	degrees
reflected radiation	R_o	$.998R_o$	$.993R_o$	$.983R_o$	$.970R_o$	$.954R_o$	$.934R_o$	$.910R_o$	$.883R_o$	
radiation difference (t_o-t_i)	0 0	$.002R_o$ 0.2	$.007R_o$ 0.7	$.017R_o$ 1.7	$.030R_o$ 3.0	$.046R_o$ 4.6	$.066R_o$ 6.6	$.090R_o$ 9.0	$.117R_o$ 11.7	per cent
radiance difference $R_o \sim 255$	0	0.5	1.8	4.3	7.6	11.7	16.8	23.0	29.8	digital counts
radiance difference $R_o \sim 240$	0	0.5	1.7	4.1	7.2	11.0	15.8	21.6	28.1	digital counts

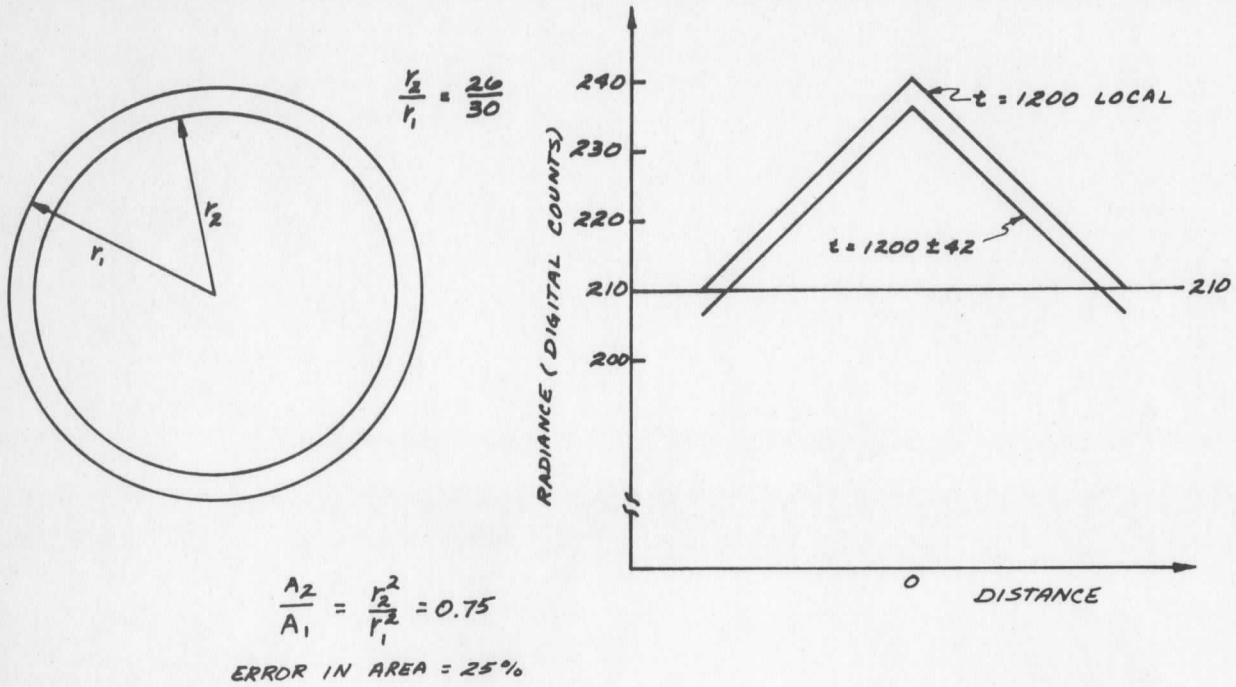

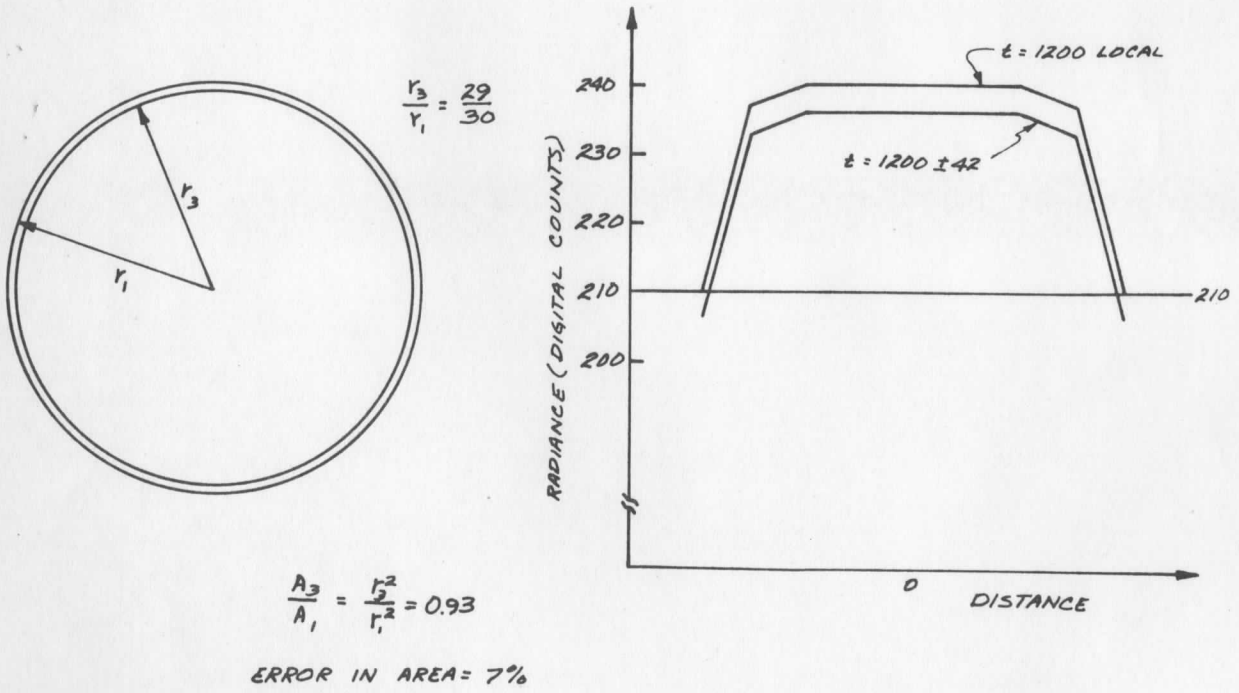

RADIANCE MODELS OF A DEEP CONVECTIVE CORE

Figure 7. Radiance models of deep convective clouds - cone-shaped radiance profile (upper) and truncated radiance profile (lower).

We assume a time difference of 42 minutes. The cloud top has its highest radiance (240 digital counts at t = 0) at the center. Radiance decreases linearly 30 digital counts from cloud center to cloud edge. With this as a radiance model, the real (radar) cloud edge will correspond to a contour of 206 digital counts, and use of the 210 contour to depict the cloud will result in radius error of 1-26/30. The error in area will be $1-26^2/30^2 = 0.25$ or 25%. However, we know from line plots across convective clouds that the cone shaped radiance distribution is unrealistic. Typically, cb radiance profiles have flat peaks and steeply sloping sides (Figure 2). If this type of profile is assumed the radius error more typically will be 1-29/30 m and the area error $1-29^2/30^2 = 0.07$ or 7%. This analysis indicates that uncorrected ATS pictures can be used to study time changes in convective activity over a three to four hour period around local noon. Beyond these limits the cosine effect will dominate changes in cloud brightness arising from meteorological mechanisms.

Normalization

The study of cloud systems in satellite photographs would be vastly simplified if each cloud could be viewed under an identical radiation geometry. This equalization of incident and reflective conditions is called normalization. The simplest normalization applies a cosine law correction to the measured radiance of clouds, in effect moving the sun to a position directly over each cloud, which is assumed to be a Lambertian reflector. A more complex scheme, advanced by Taylor (1970), corrects for the solar zenith angle by an empirical normalization derived from ATS 1 pictures. Marshall and Vonder Haar have assembled tables of cloud radiance values to generate an empirical normalization for solar and satellite zenith and the relative angle between satellite and sun (Vonder Haar and Cram, 1971).

The crucial limitations of these schemes for the present study are their lack of corrections for cumulonimbus clouds <u>per se</u>, and the large effort and expense required for each normalization. For studies involving data in the amounts used

here the normalization must be done quickly and cheaply, for example, through an analog device inserted between the tape transcriber and enhancement box of the ATS precision display system.

With this in mind, a program was developed to determine the brightness characteristics of deep convective cloud tops as a function of solar and satellite zenith and satellite-solar relative angles. The program was predicated on the assumptions that (1) tropical deep convective clouds are virtually identical in their reflective properties, (2) all cloud clusters of a certain appearance contain one or more deep convective clouds, and (3) deep convective clouds are brighter than other clouds, whatever the sun-cloud-satellite geometry. If these conditions are satisfied, frequency distributions of radiance for cloud clusters will have two primary components - deep convective clouds and all other clouds - with the upper part of the distribution reflecting the contribution of deep convective clouds. A series of such distributions for a number of solar and satellite zenith angles will show the real change of cb brightness over varying configurations of radiation geometry.

The first plottings of maximum digital count as a function of solar zenith suggested the hypothesis is sound; however, lack of suitable tapes has precluded a thorough evaluation. The primary limitation on data tapes is signal saturation within clusters. Where gains were low enough to prevent saturation variable camera and ground station gain settings complicated the analysis. The result is that only the effect of solar zenith angle can be discussed with any confidence.

The procedure followed was to first locate a series of three or more ATS data tapes, either analog or digital, for a single day. Convectively active cloud clusters were isolated on pictures, then located on the tapes using either a photo facsimile readout of portions of the tapes or a record-element overlay superimposed on the picture. Segments of the data tape corresponding to selected clusters were run on a program that produced a frequency distribution of brightness digital count. These distributions, because of varying meteorological conditions, as well

as data selection, sometimes did not show the expected bimodal curve. Since suitable tapes were in short supply, maximum digital count, which could easily be read from such distributions, was selected for analysis rather than other distribution properties such as the mean or modal value which could not. In a few cases parity errors or noise on the tape produced a discontinuous distribution. A tape found to have substantial noise or more than a few parity errors was discarded. If an otherwise good tape produced a distribution having an interval of four more digital counts between an isolated upper point and the rest of the distribution, the second highest point was used in the analysis.

A search of the entire ATS library and screening of candidate tapes by the method outlined above produced a basic data set which was divided into three categories - pre-BOMEX, BOMEX, and post-BOMEX (Figure 8), according to whether it was known with reasonable confidence ground station gains had been held constant between documented changes (BOMEX), ground station changes had been adjusted without documentation from time to time (post-BOMEX), or ground station gains may have been adjusted without documentation (pre-BOMEX).* For a study of this type the size of the basic data set is definitely a limiting factor.

The problem of different camera and ground station gain setting combinations was solved by referring all digital values to a standard 3, 8 gain. This was accomplished through data on gain setting ratios for camera and ground station available in the Technical Data Report for ATS (1968).

Results for the better tapes are plotted in curves of maximum digital count as a function of solar zenith angle (Figure 9a, b, c, and d). Since each cloud cluster is plotted separately, the effect of satellite zenith angle is also evident. Most striking about the graphs is a strong resemblence to the change predicted by the cosine law; however there is a small leftward displacement of the empirical

---

* All tapes are ATS III; tapes from ATS I contained an unacceptable level of saturation.

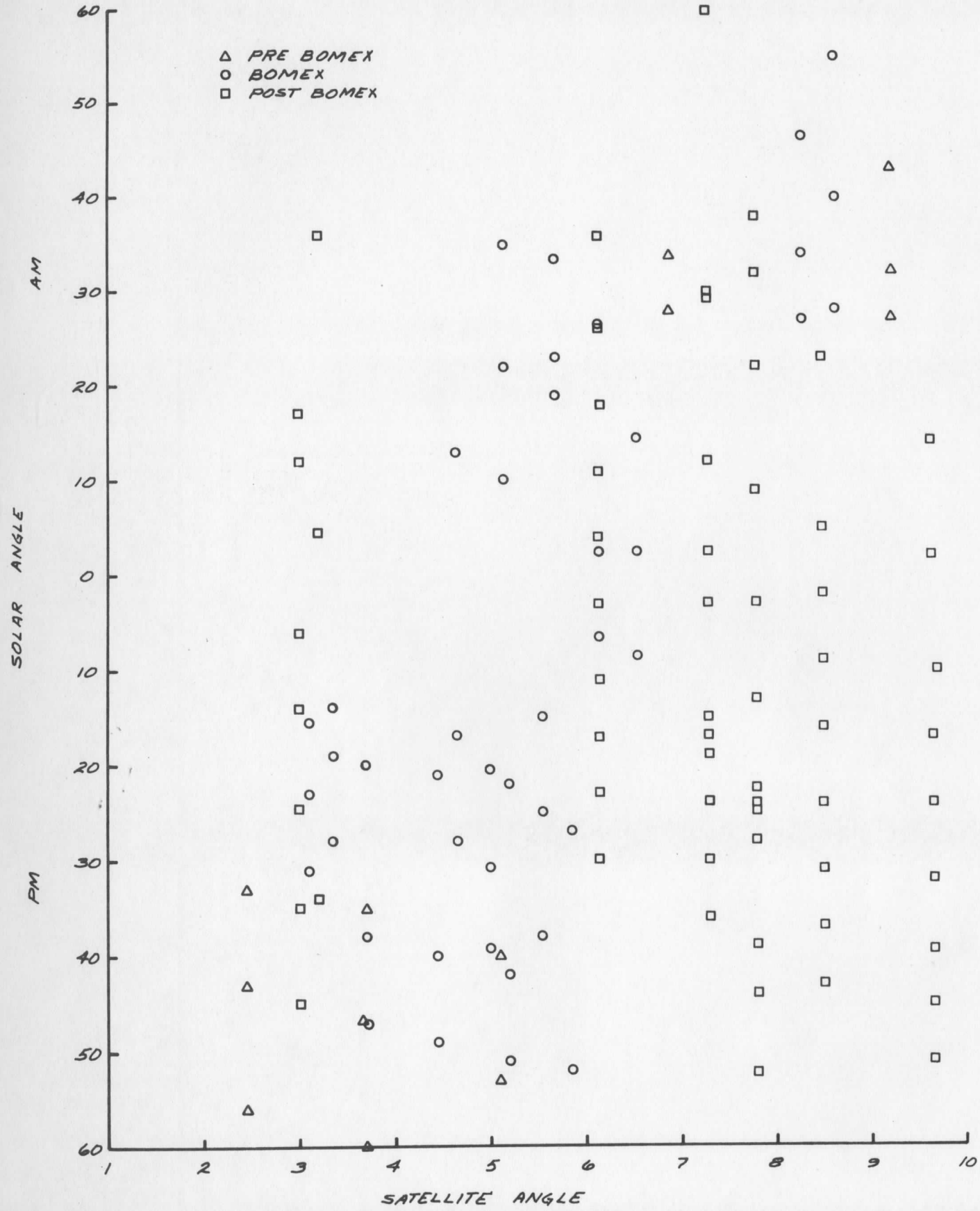

Figure 8. Data available for development of an empirical normalization. All suitable cloud clusters on each acceptable picture tape are plotted according to the satellite zenith angle and the solar zenith angle.

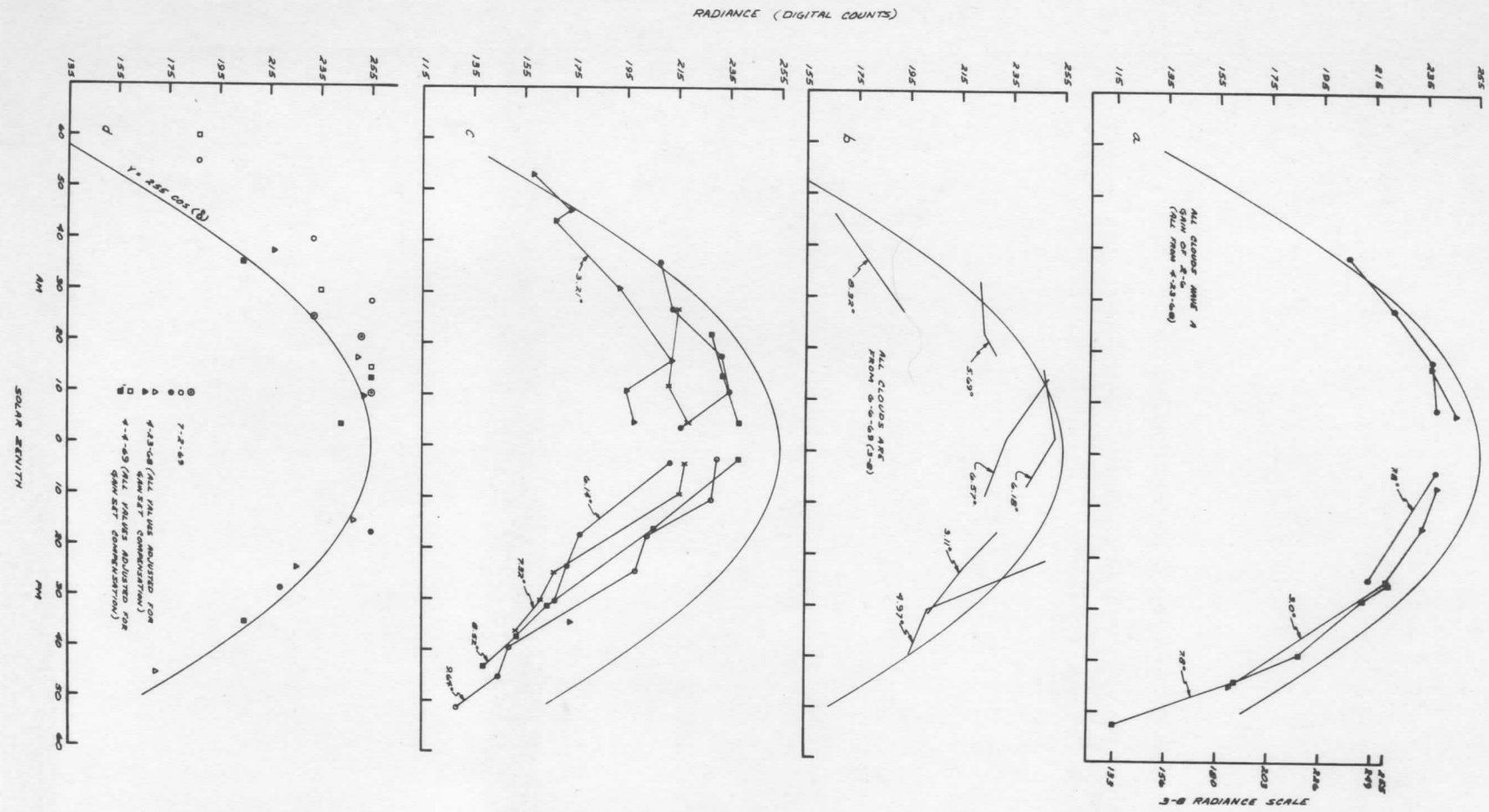

Figure 9. Maximum digital count as a function of the solar zenith angle (δ). Each line in (a), (b), and (c) represents a single cluster followed through a series of pictures. Points in (d) are for individual clusters. Numbers adjacent to lines give the satellite viewing angle. The cosine law change of incident radiation as a function of solar zenith angle is included for reference. Part (a) 23 April 1968; part (b) 6 June 1969; part (c) 4 April 1969; part (d) 2 July 1969, 23 April 1968, and 4 April 1969.

curves relative to the cosine curve. The sense and amount of this displacement is such that maximum digital counts are reached 20 min. before local (cluster) noon.

Also apparent, especially in part (c) of Figure 9, are rather large differences in maximum digital count for different clusters. This probably is due to varying intensities and vertical extent of deep convection from cluster to cluster. Low digital counts at high solar zenith angles are indicative of a non-convective cluster; the lowest curve in part (c) may fall in this category.

This very small sample suggests that changes due to the satellite viewing angle are small, at least through ranges of the solar zenith angle up to 30°. Since the form of curves of maximum radiance closely resembles a cosine function, over this angular range the assumption of Lambertian reflectance for cumulonimbus tops is valid.

Real Time ATS

The Space Science and Engineering Center is one of three users able to receive real time ATS I and ATS III picture transmissions from the Wallops ground station via the Environmental Satellite Center. Because a primary use of real time ATS is identifying and monitoring convective storms, a part of this study is concerned with the application of enhancement techniques to the real time signal. It is realized that the operational requirements of other users contribute to the signal specifications; the point of this discussion is to suggest that the enhancements that have been adopted may be incompatible with the use of this technique to isolate convection.

First applications of the case 4 transfer function to the real time signal failed utterly to isolate convective clouds. The reasons for this failure became apparent as enhancements applied at the ground station and again at the Environmental Satellite Center were examined. (Figure 10). These enhancements virtually eliminate the upper 35 % of the original signal. Since deep convective cores near the solar subpoint will at nominal gain settings occupy the upper 10 to 15 % of

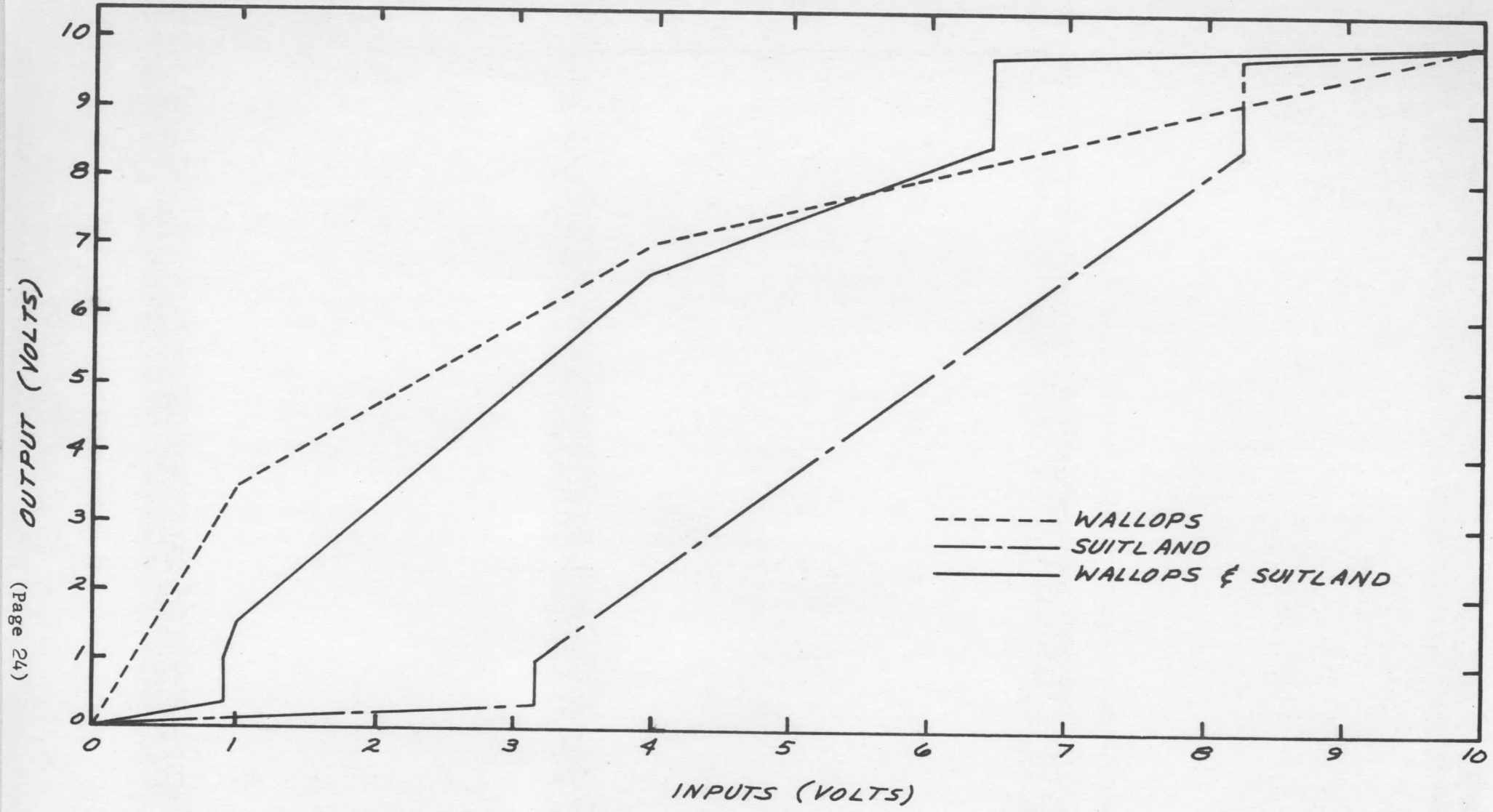

Figure 10. Enhancement curves applied to the real time ATS signal at the Wallops Island ground station and Environmental Satellite Center at Suitland, Maryland, as of 16 March 1971.

the total brightness range, the ground station and Satellite Center enhancements precluded isolation of deep convection by any method.

A further complication discussed previously is variable, unknown ground station gains. It has been pointed out before, but bears repeating: to the extent that ground station gains are not known the data are useless for quantitative work.

One of the reasons given for adding the enhancements is the avoidance of noise on the transmission line. However, on 21 July 1971 engineers at SSEC measured a signal to noise ratio of 44-db on the real time line. This suggests that the pure ATS signal could be transmitted with very little loss of information. If each user were equipped with an enhancement box the requirements of one would in no way interfere with the requirements of the others.

III. Analysis

Census

Method and data

The cloud census covers the Atlantic Ocean from Africa to South America. This area was divided into three approximately equal regions (Figure 11), each of which was considered separately in parallel censuses, one of cloud clusters made from daily ESSA and ITOS digital mosaics supplemented by ordinary ATS pictures, and the other of bright spots appearing in enhanced ATS pictures.

For each day during June and July 1969 and July, August, and September, 1970, ESSA and ITOS mosaics and/or conventional ATS photographs were examined for cloud clusters larger than 1 deg^2. All such clusters, excluding those obviously composed only of low level stratiform clouds, were numbered, measured to the nearest degree squared, recorded by region, and tracked from day to day until they dissipated or moved outside the area of interest. Disturbances moving into the eastern region from Africa were tracked back in time to their beginning. Statistics computed from these data are total number of disturbances (each disturbance counted once per day), average area, and average lifetime. Lifetimes are divided into two categories: those for systems dissipating within the area of interest, and those for systems moving out of the area of interest.

Each suitably enhanced ATS photograph was examined for bright spots. The areas of these bright spots were measured to the nearest tenth of a degree squared using a one degree by one degree transparent grid. Assemblies of bright spots representing individual clusters were treated as entities in the statistics, although no effort was made to refer these directly to clus-

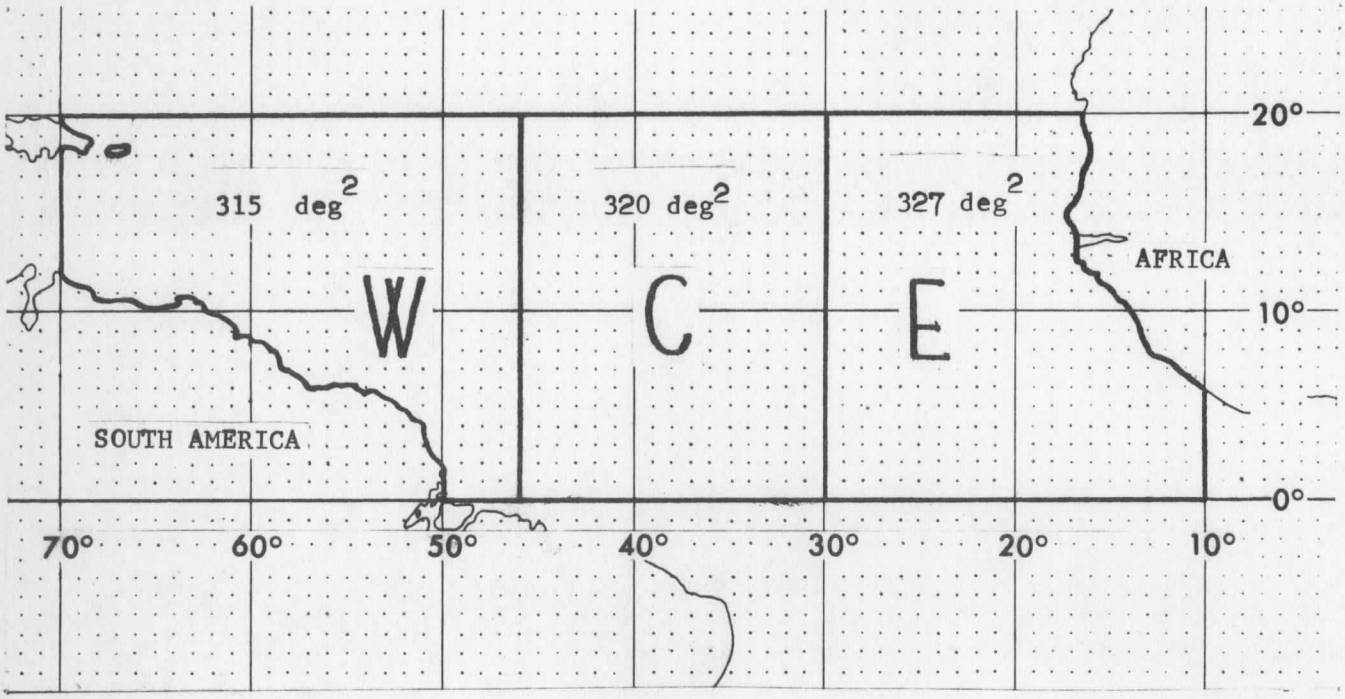

Figure 11. Map of the study area and subregions into which it is divided. Numbers above each letter label (W = west, C = central, E = east) give the area of the subregion.

ters defined in the conventional census. (For a clarification of nomenclature see Figure 12.) Areas were recorded separately for each of the three regions. In general, if the subsolar point was more than 30° degrees from the central longitude of a region that photo was not used to measure areas of bright spots in the region. Analog tapes suitable for enhancement were available in quantities sufficient for a census of the following months:

Jun	1969	21 days
Jul	1969	11 days

Results

The 1969 and 1970 cluster census (Table 2 and Figure 13) indicates greater numbers of clusters in the eastern Atlantic in June, 1969. In July of both years highest frequencies are found in the western Atlantic; in August and September 1970 frequencies are similar for all regions. Western clusters are in every case but one 25 to 50 per cent smaller than those in eastern and central regions. Areas increase by 75 per cent from July 1969 to July 1970 in the central region. Smaller increases were recorded for the west and east Atlantic. Variability from month to month is substantial, especially in the west and central regions. Except in the west it is greater for average area than for number of clusters.

Lifetimes of these Atlantic clusters (Table 2) are somewhat longer than lifetimes of Pacific clusters studied by Martin and Karst (1969), and substantially longer than mean lifetimes found by Frank (1970). This long average lifetime in part is due to origins for many clusters well within the African continent and tracks that carried systems westward through each of the subregions. The use of ATS pictures as supplements to once daily ESSA and ITOS digital mosaics and a less restrictive definition of cloud cluster for the present study may account for differences between lifetimes found here and those found by Frank.

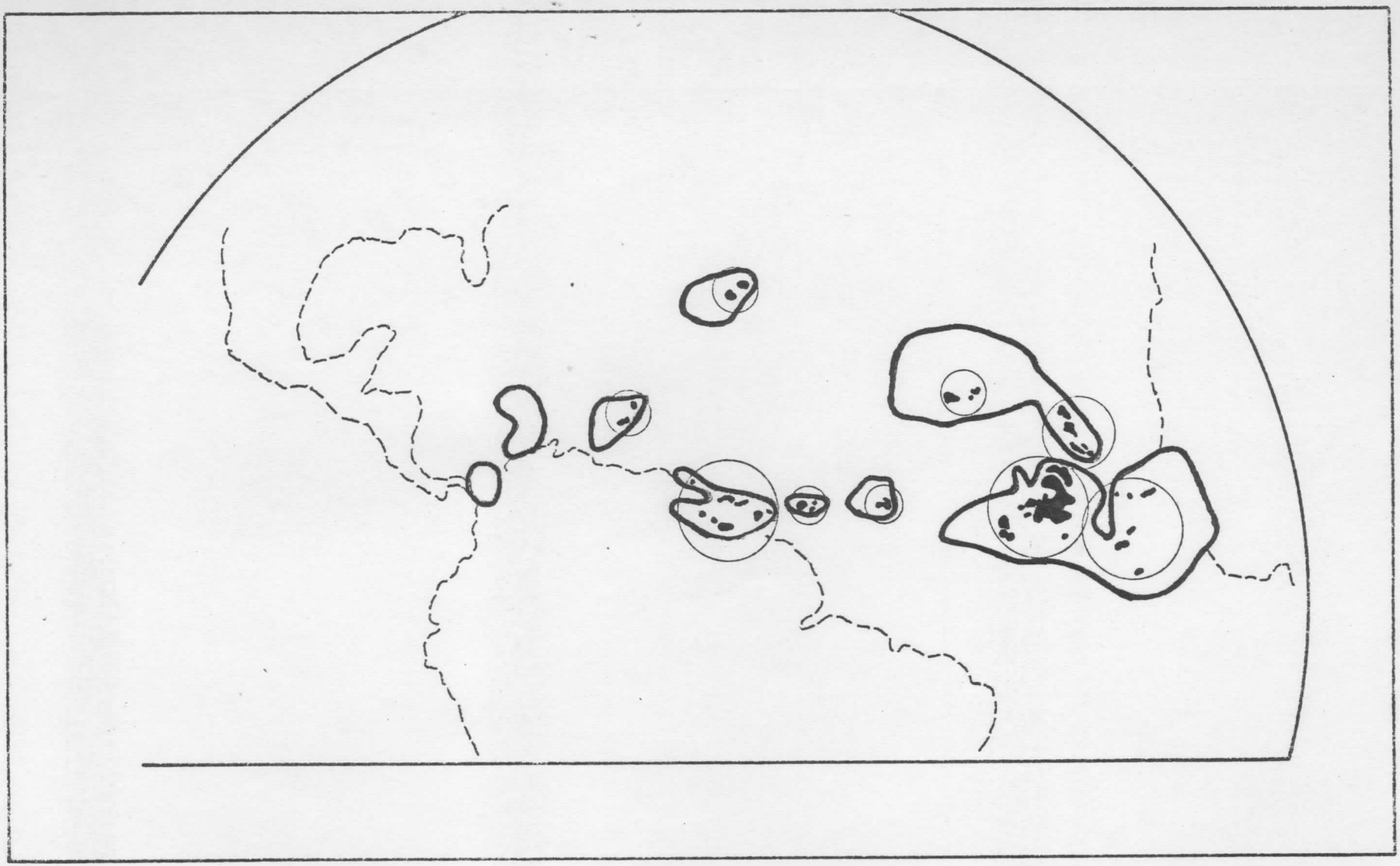

Figure 12. Bright spots are represented by solid areas and cloud clusters by heavy lines in this abstraction of an enhanced ATS image. Spot assemblies are circled.

TABLE 2. AREAS OF BRIGHT SPOTS AND CLOUD CLUSTERS

			NUMBER OF CLUSTERS-ALL DAYS	AVERAGE AREA OF CLUSTERS-ALL DAYS deg^2	LIFETIMES OF CLUSTERS: DIED INSIDE days	LIFETIMES OF CLUSTERS: DIED OUTSIDE days	NUMBER OF CLUSTERS-SELECTED DAYS	TOTAL AREA OF SELECTED CLUSTERS deg^2	AVERAGE AREA OF SELECTED CLUSTERS deg^2	NUMBER OF BRIGHT SPOT ASSEMBLIES	TOTAL AREA OF BRIGHT SPOT ASSEMBLIES deg^2	AVERAGE AREA OF BRIGHT SPOT ASSEMBLIES deg^2	RATIO-TOTAL AREA SPOT ASSEMBLIES TO TOTAL AREA SELECTED CLUSTERS
JUN	69	E	49	40			21	796	38	23	145.9	6.3	0.18
		C	30	37			18	784	43	29	132.6	4.6	0.17
		W	38	31			22	705	32	43	116.6	2.7	0.17
		all			4.3	5.2							
JUL	69	E	47	44			12	413	34	12	75.1	6.3	0.18
		C	37	37			16	550	34	18	75.3	4.2	0.14
		W	57	24			18	366	20	14	29.4	2.1	0.08
		all			3.8	4.9							
JUL	70	E	55	57									
		C	45	64									
		W	60	42									
		all			3.7	4.4							
AUG	70	E	53	55									
		C	54	57									
		W	47	41									
		all			3.5	6.0							
SEP	70	E	56	45									
		C	55	29									
		W	52	27									
		all			3.4	5.6							

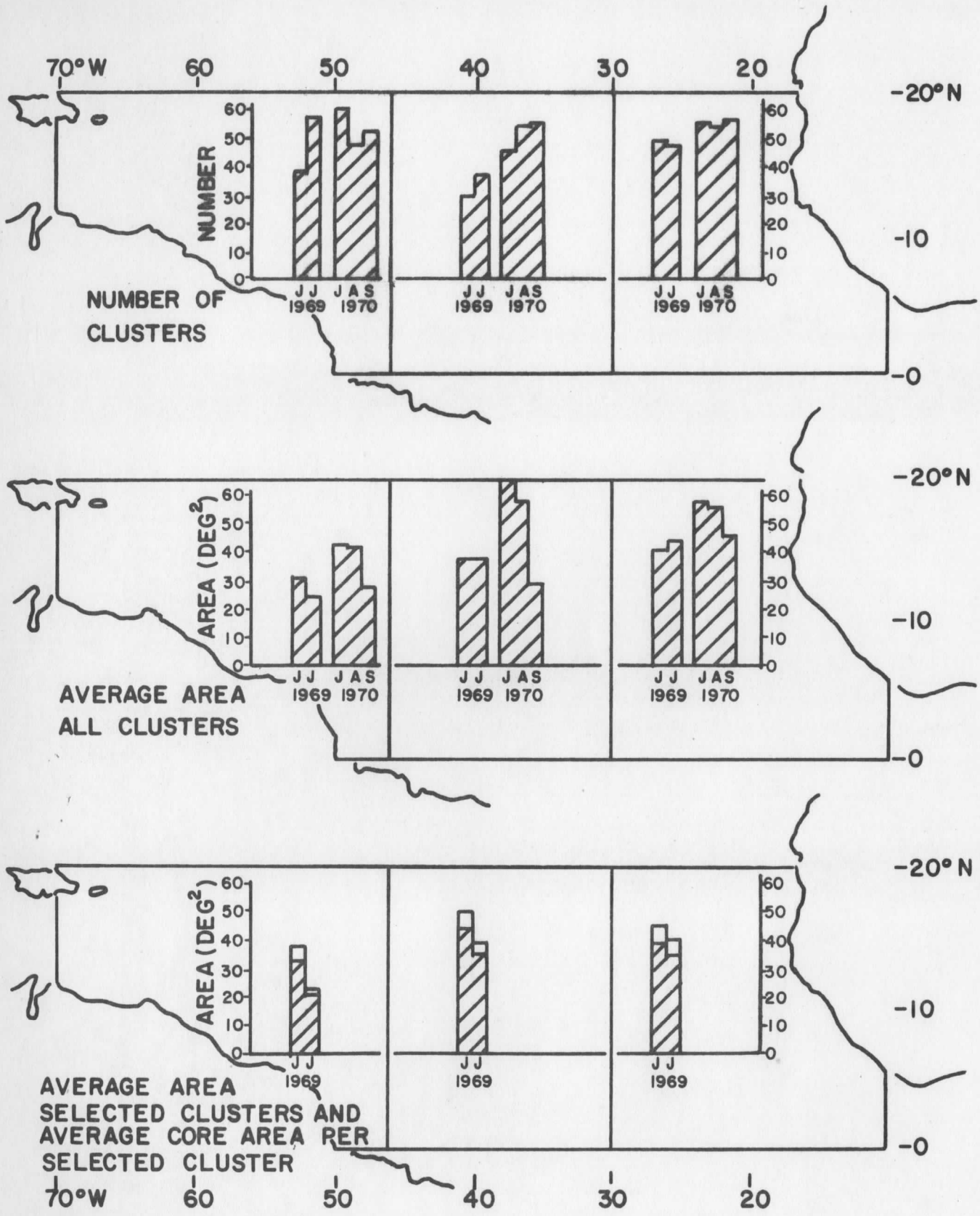

Figure 13. Cluster frequencies, areas, and convective activity for three regions of the Atlantic.

The ratio of bright spot area to cloud cluster area is a measure of convective activity within a cluster. It is computed by stratifying cluster area data according to whether or not a suitable enhanced picture was available for a subregion during June and July, 1969. Hence, while there is no necessary correspondence between bright spot assembles and cloud clusters, no clusters are included in the ratio which do not appear in the enhanced ATS pictures from which bright spot areas were measured. These ratios vary from 0.1 to 0.2. There is little change across the Atlantic in June; however, a sharp decrease occurs in the western Atlantic in July.

Plots of bright spot area from day to day (Figure 14) show pronounced variations; therefore, the decline in spot area in the west in July may in part be a result of poor sampling.

Complete day series of enhanced pictures show on three days the longitudinal and latitudinal concentration of bright spots (Figure 15a, b and c). These curves were obtained by assuming that the total area of a spot, measured on the picture nearest local noon for the spot, is concentrated at the latitude or longitude of its center. Spot areas were then totalled for one degree strips of latitude and one degree strips of longitude.

On the 22nd of July 1969 (Figure 15a) cores were concentrated between 7 and 14°N. Longitudinally, the distribution was much broader, extending over twenty degrees. This is probably a typical active ITCZ distribution for the eastern and central Atlantic.

Plots for two consecutive days in 1970 (Figure 15b and c) show peaks associated with distinct clusters and the movement of these clusters over the interval. On 21 August 1970, an inactive cluster lay just off the coast of Africa. This cluster has moved slightly westward and had intensified its convective activity by picture time the following day. The more active mid-Atlantic cluster showed a similar movement but an opposite trend in convec-

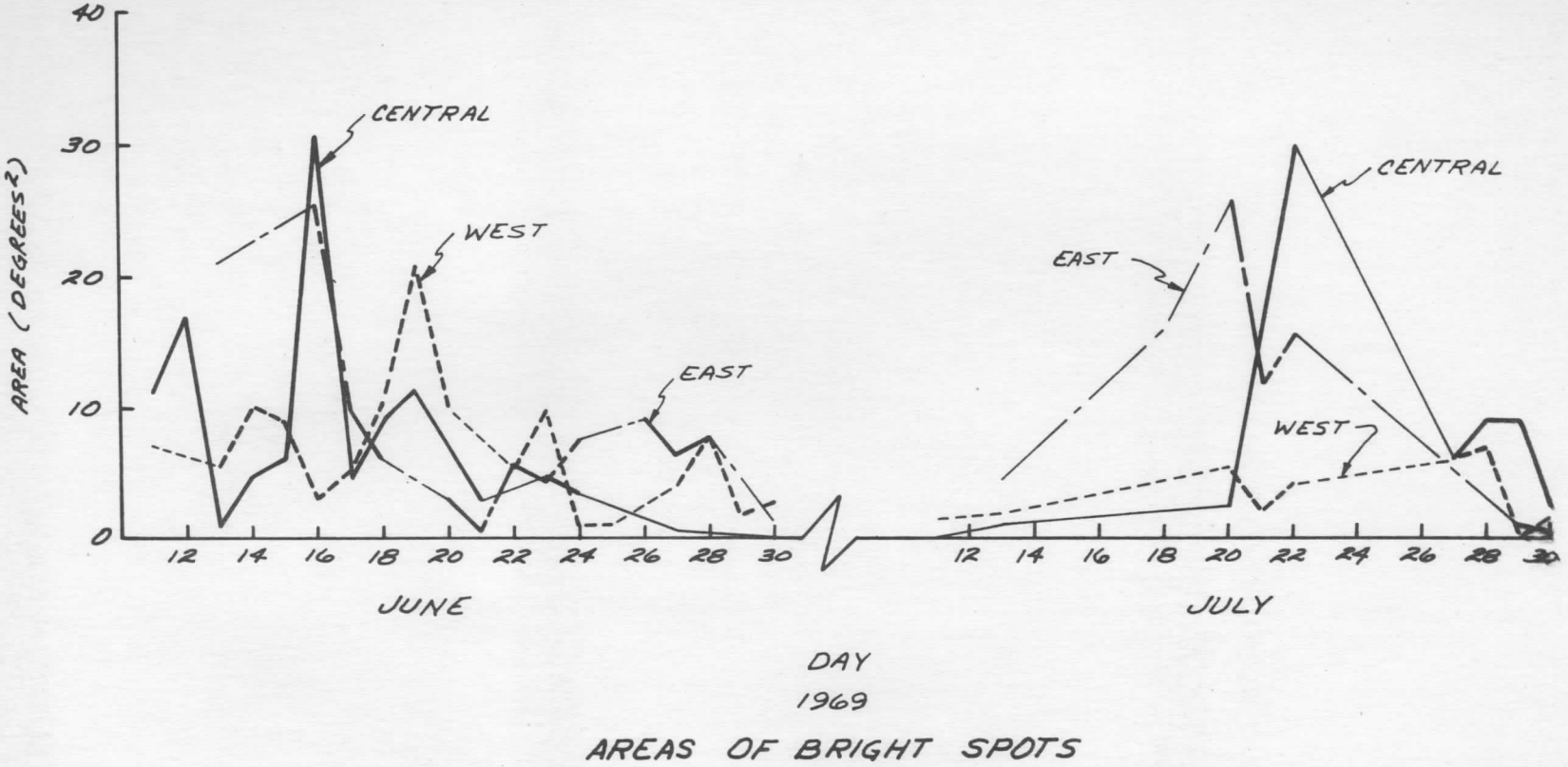

Figure 14. Daily change in the total area of bright spots for east, central, and west regions of the tropical Atlantic. Thin lines bridge gaps of one day or longer in the data series.

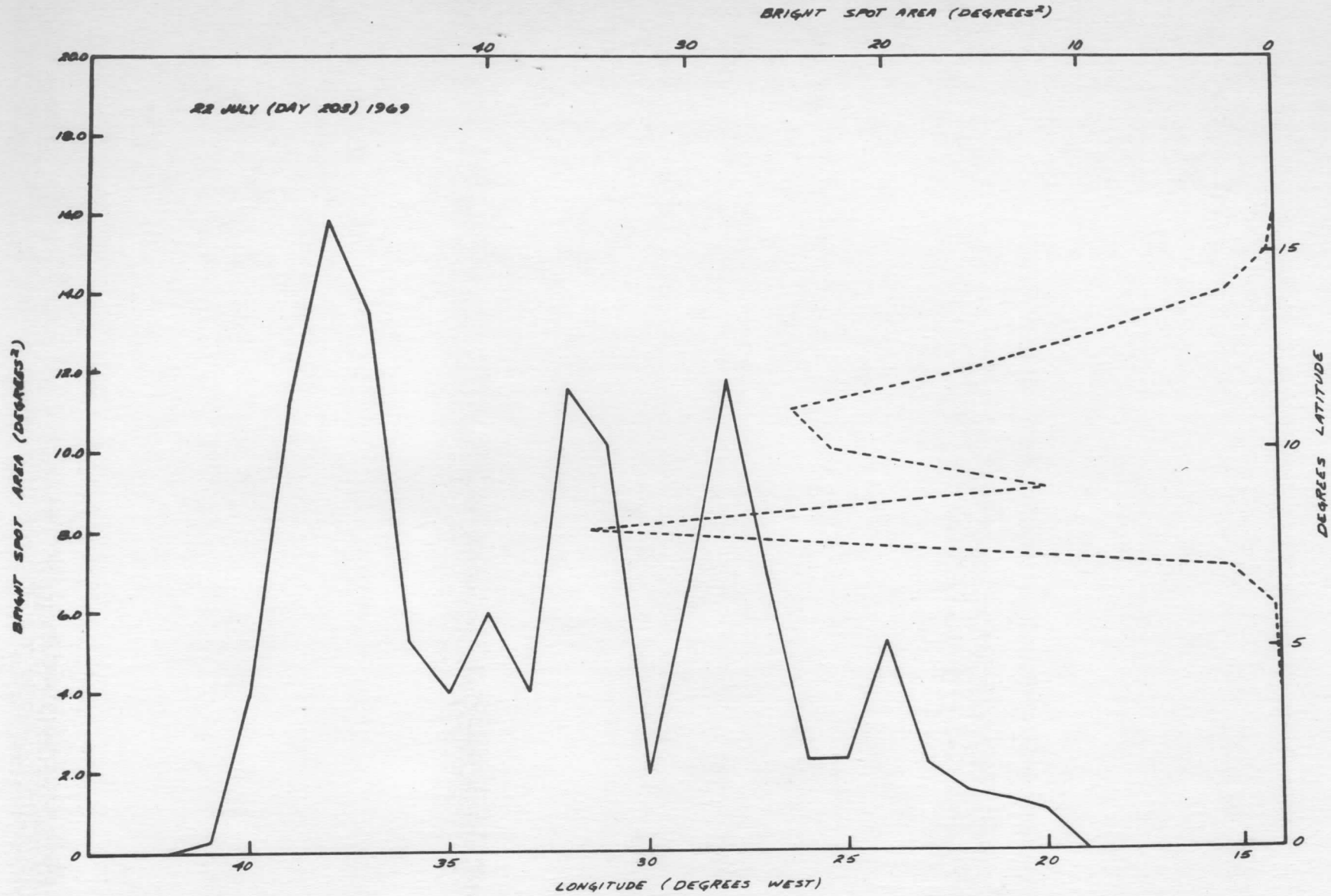

Figure 15.a Areas of bright spots totaled for one degree strips of latitude and longitude. 22 July 1969.

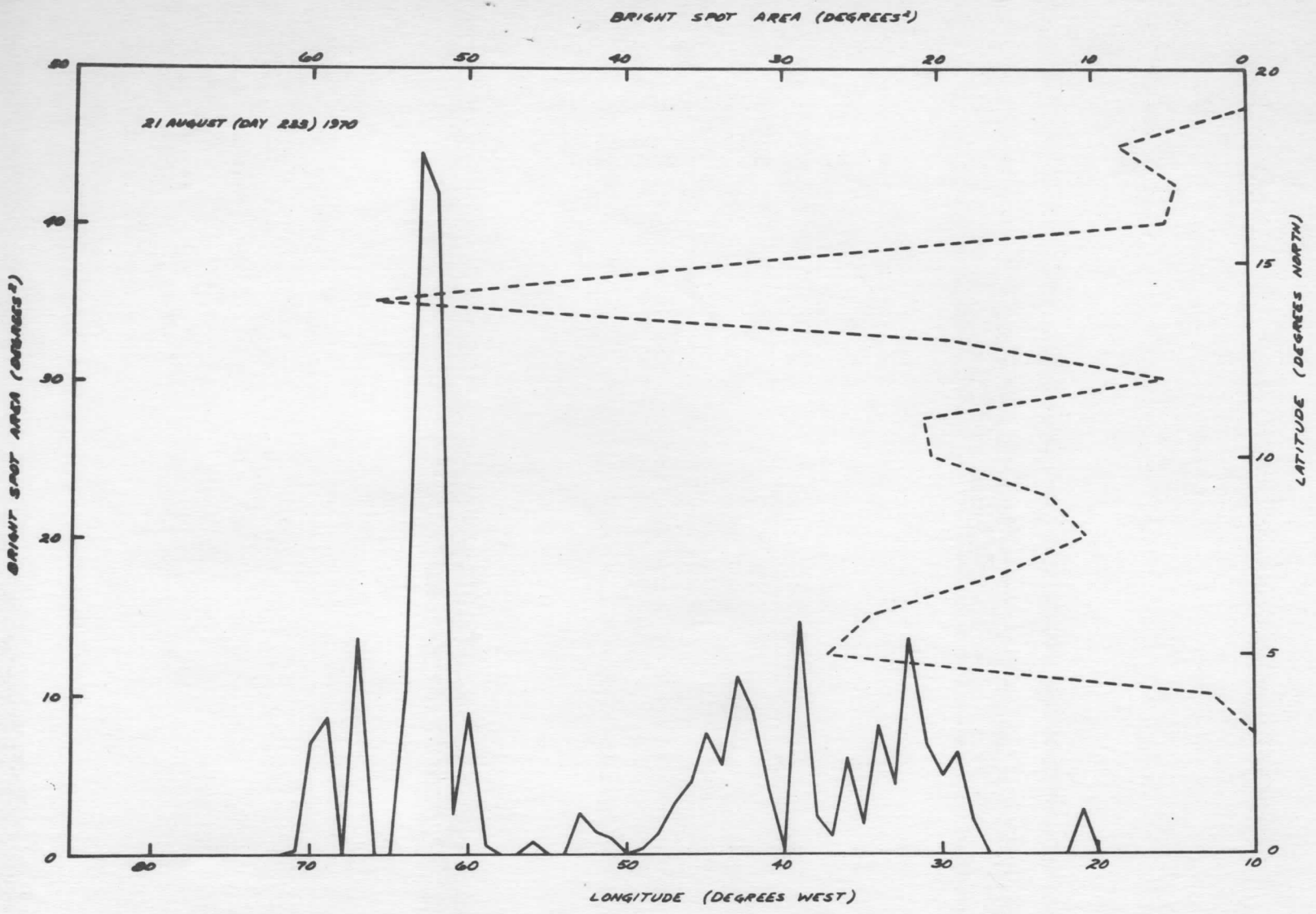

Figure 15.b As for 15.a, except 21 August 1970.

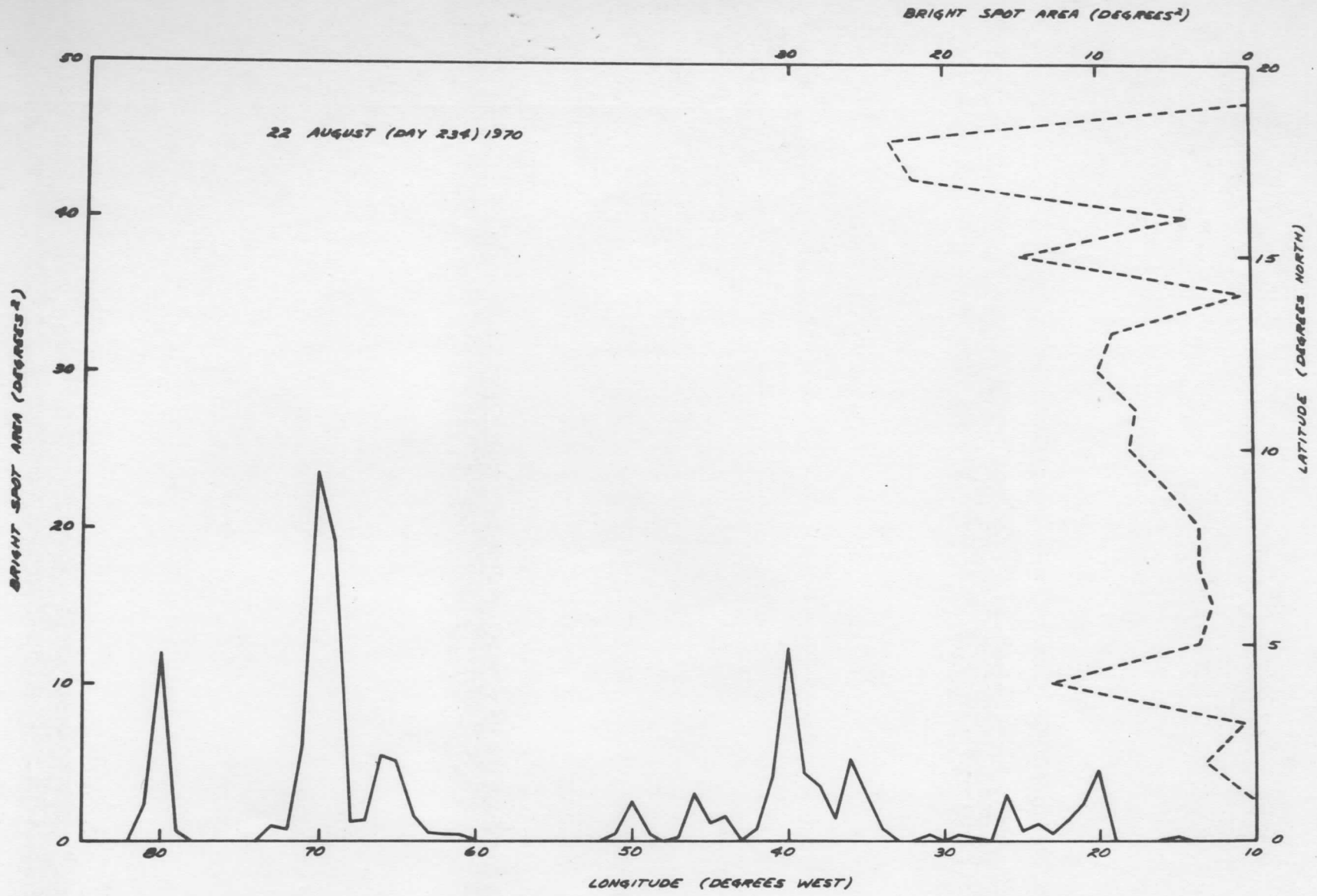

Figure 15.c As for 15.a, except 22 August 1970.

tive activity. The pronounced peak in core area at 13 to 15°N on the 21st reflects intense convection in a cluster just north of Trinidad. Activity of this cluster diminished markedly as the system moved northwestward into the Caribbean Sea.

After pictures for August and September 1970 had been processed, it was learned that at the ground station gain adjustments made from picture to picture were not documented. Since the typical pattern of adjustment was to raise gains early in the satellite morning and lower gains near satellite noon (Gage, 1971), area comparisons would suffer from a bias of unknown but probably substantial magnitude. Because of this uncertainty the results of the 1970 bright spot census are withheld; however, results from three complete day pictures series are presented. The nature of the series and the inferences made from them together with the apparent absence of substantial gain changes as evidenced by densitometer traces for three of the four days (Figure 3a, b, c) suggest no contamination of these results.

ATS - BOMEX Radar Comparisons

Radar

The operation of two ground based meteorological radars during BOMEX offers an unparalleled opportunity to find out precisely what the enhanced ATS picture portrays. One of these radars, an AN/MPS-34, was located on the island of Barbados at 13° 12′N, 59° 32′W (Hudlow, 1970); the other, a Selenia Meteor 200 RMT - 25, was mounted on board the U. S. Coast and Geodetic Survey Ship Discoverer which was in a station keeping mode at 13° 08′N, 54° 51′W (BOMEX Bulletin No. 3, 1969). Both radars operated in the X - band (3 cm), with antenna elevation at a nominal 0°.

Through the BOMAP office radar images were obtained for selected times on seven days in July 1969. A small number of these images were enlarged for comparison with near simultaneous ATS data. Within the constraint of no more than five minutes difference between radar and ATS imaging times (eight minutes added to ATS picture times to account for the difference between picture start time and scan time across the BOMEX network) picture selection was governed by availability of good digital tapes and echo activity in near simultaneous radar displays.

ATS

Projection differences severely limited direct comparisons of ATS with radar images. Conversion of ATS to a suitable projection was accomplished by navigating a digitized magnetic tape of the ATS picture using the program of Phillips and Smith (Reference Manual for ATSLIB, 1971). An area enclosing the Barbados or Discoverer radar image was isolated on the navigated tape and run through a mapping program which converted the data array to an azimuthal (Gnomonic) projection having Barbados or the Discoverer at the origin. Output was a contoured map of digital brightness, on very nearly the same scale and projection as the enlarged radar image.

Error analysis

First comparisons of radar and ATS images showed almost one to one agreement between small echoes and small, isolated clouds. The coincidence was so good these echoes were used to renavigate the ATS pictures, by shifting the ATS image until the patterns of small echoes and small clouds were superimposed. (This method could be used as a basis for navigating the entire ATS picture, since the latitude and longitude of an echo and hence the corresponding cloud is known quite precisely from the radar image. One tape used in the present

study was successfully navigated a second time by this method. Conceivably, small clouds geographically fixed by radar may entirely replace landmarks in the navigation of ATS cloud images for advanced programs such as wind estimation by cloud displacement, an application suggested by Phillips [1971]).

Renavigation reduced variation of radar and cloud patterns; however, other error sources remain rather large. These include distortions in the original ATS and radar images, measurement errors in determining scaling, enlargement errors, and uncertainty in the location of the Discoverer. The latter could be important where isolated small clouds are absent and the ATS navigation error itself is large. A phasing problem in the Discoverer radar in at least one picture produced misorientation between the image azimuths and bezel azimuths. Because of distorting and scaling errors agreement on a point-to-point basis is good at best over limited areas of the image. Rapid changes in cloud patterns led to discrepanicies in spite of time differences no larger than minutes. A poor choice of low level contour sometimes resulted in echoes finding no cloud counterpart on the ATS image; the opposite situation, clouds where no echoes were visible, could at times be accounted for by beam undershoot or overshoot. Anomolous displacement between cloud contour and echo observed occasionally might have been caused by shearing of a cumulus cloud.

Results

ATS - radar comparisons are presented in Figures 16 to 25. They cover a total of six ATS pictures on three days in July 1969.

The first of these comparisons, for Discoverer at 1402Z (ATS) 1410Z (radar) (1026/1034 local) on 22 July (Figure 16), demonstrates the striking coincidence which typically was observed between small echoes and small clouds. With

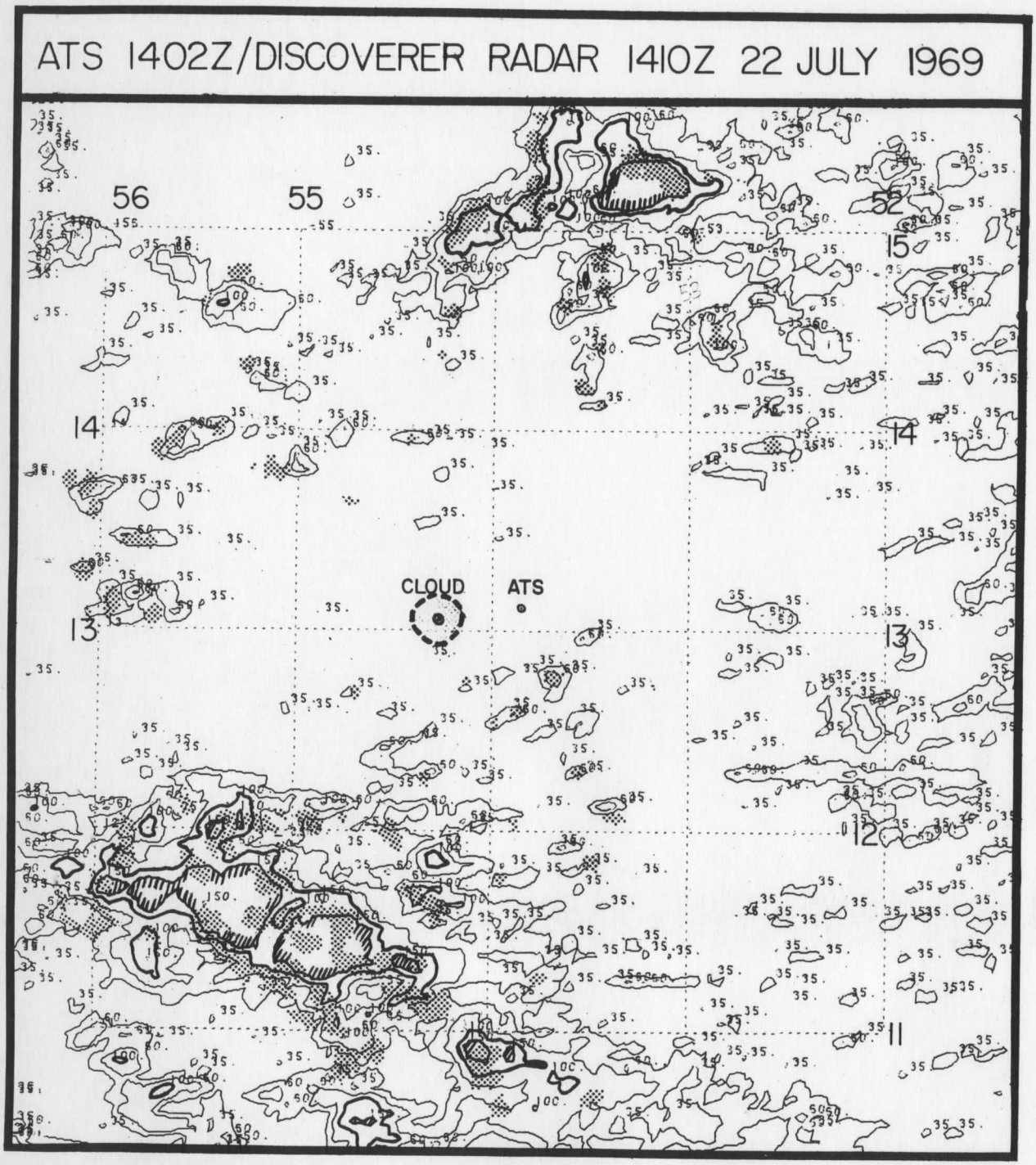

Figure 16. Contours of digital brightness from ATS III with Discoverer radar echoes superimposed. 150 digital count contours are emphasized by hatching; 200 contours by cross hatching. "ATS" indicates radar location on the ATS image as determined by ATS navigation and specified radar latitude and longitude; "CLOUD" indicates radar position as determined by cloud and echo pattern navigation. Dashed line shows the limits of ground clutter.

the ATS image repositioned to superimpose small cloud and small echo patterns, larger echoes in the lower left and upper center are almost entirely enclosed by the 100 digital count contour. The 150 contour in almost all instances surrounds or intercepts major echoes.

The Barbados radar at about the same time - 1402/1412Z (1026/1036 local) surveyed a markedly different synoptic situation (Figure 17). Barbados was on the north edge of an active, solid cluster. Although small clouds and echoes were sparse, the patterns are in sufficient agreement for renavigation of ATS. Superimposing images on that basis again gives fine agreement between very large echoes and areas of greater than 150 digital counts, except close to the radar where a 150 contour encloses no echo.

Poor selection of contour levels hampers comparisons of the Discoverer radar and ATS at 1247/1251Z (0911/0915 local) on 26 July (Figure 18). Nevertheless the isolated clouds of 50 digital counts or greater, with one exception, have echoes counterparts. 150 contours are nonexistent; however, the few 100 contours reasonably close to the radar fall over or adjacent to echoes.

At Barbados a few minutes later - 1247/1259Z (0911/0923 local) - an extensive overcast complicates comparisons (Figure 19). In this case radar and ATS images were superimposed according to the original ATS navigation. Major cloud bands, specified by the 100 and 150 contours, coincide with echo bands. Both show a spiral banding in the system northeast of Barbados.

This disturbance was monitored an hour and a half later at 1430/1443Z (1054/1107 local). Rapid development over the interval had produced two very large echoes which are enclosed by the 150 contour (Figure 20). A 200 digital count contour, the only one observed in the series, encloses parts of both echoes and the narrow gap between. Discrepancies noted here may in part be due to a five minute difference in image time during a period of explosive convective development.

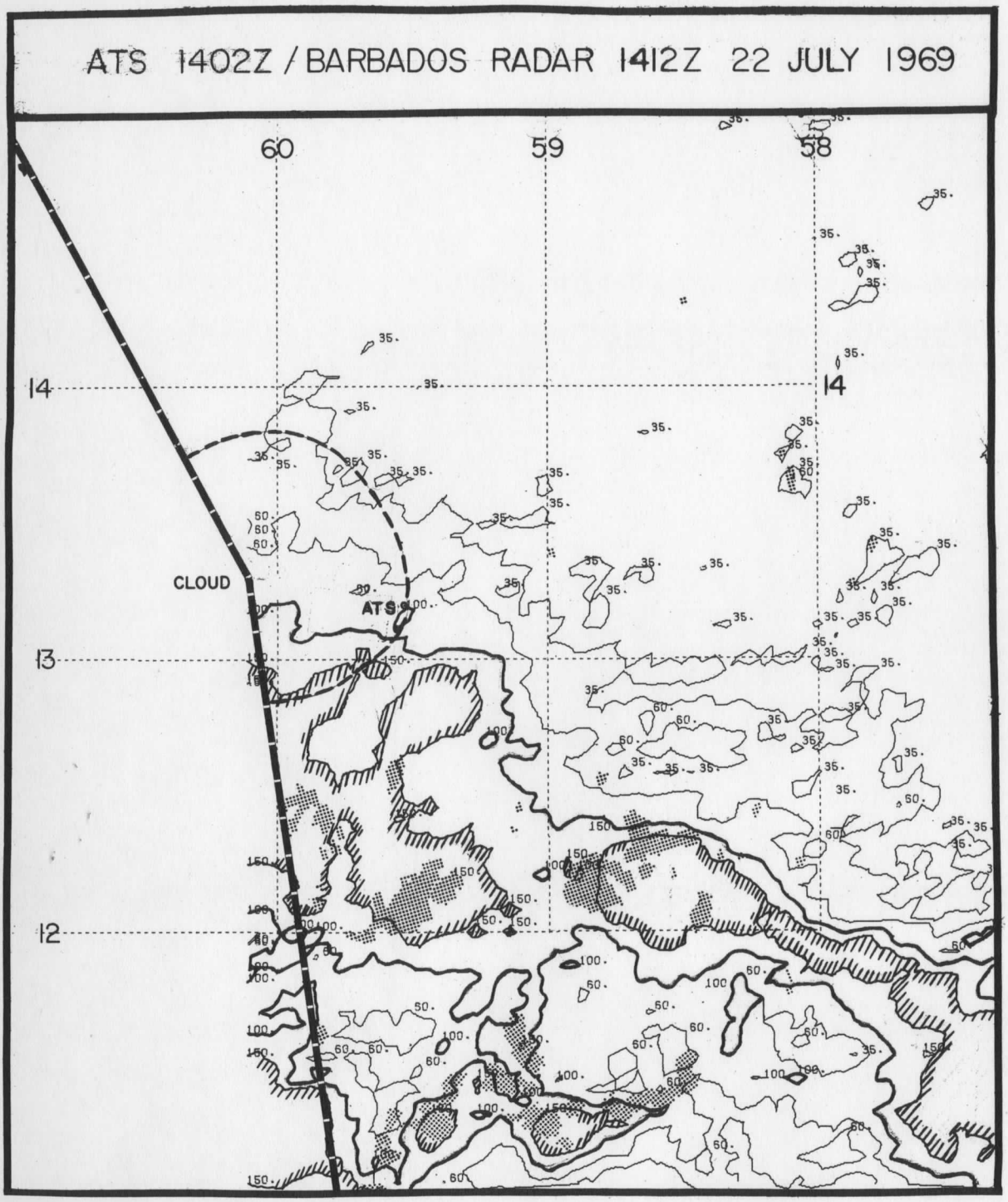

Figure 17. As for Figure 16, except Barbados radar. Cyclic elevation of the antenna resulted in almost total loss of echo information in the western sector.

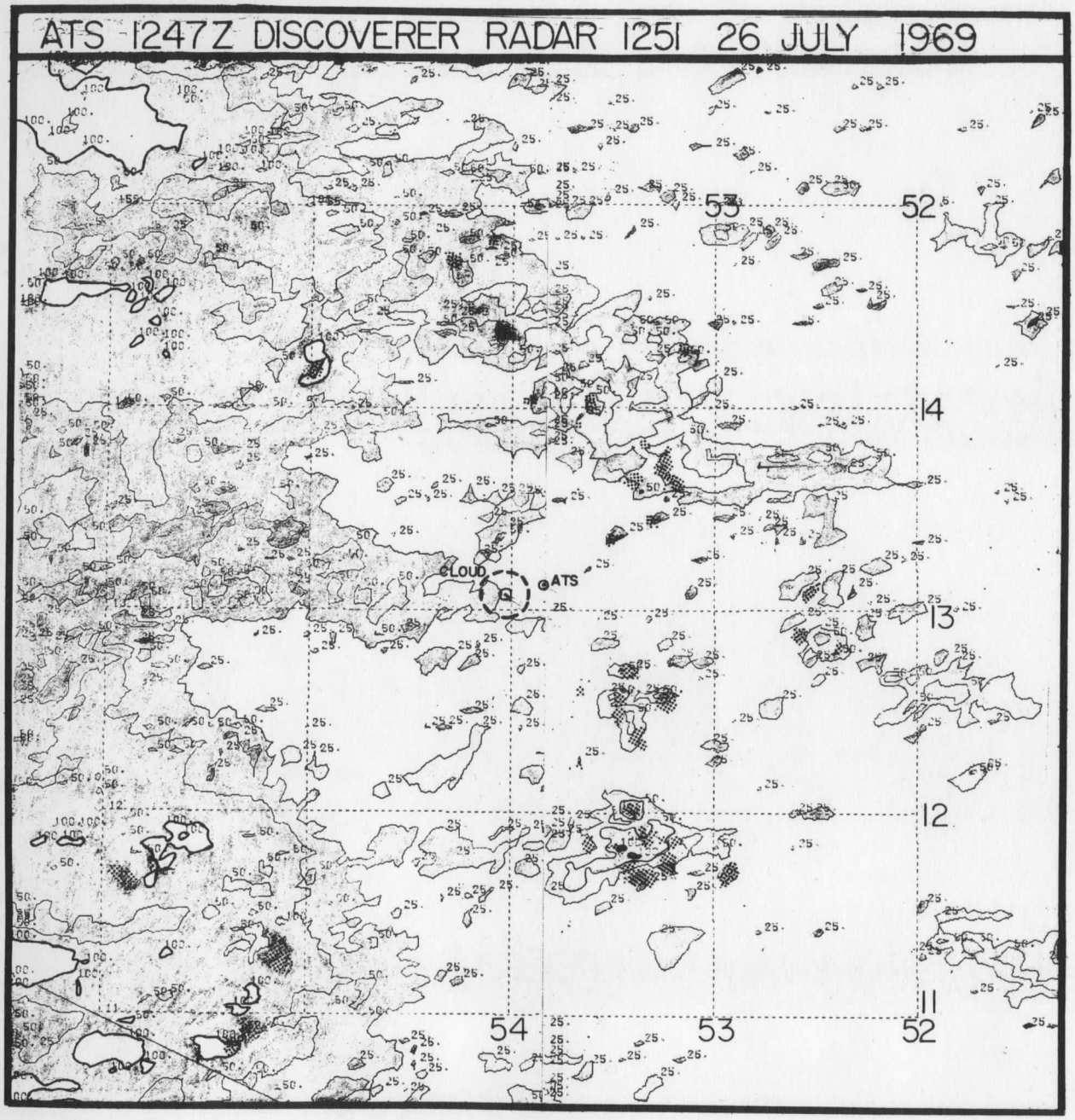

Figure 18. As for Figure 16.

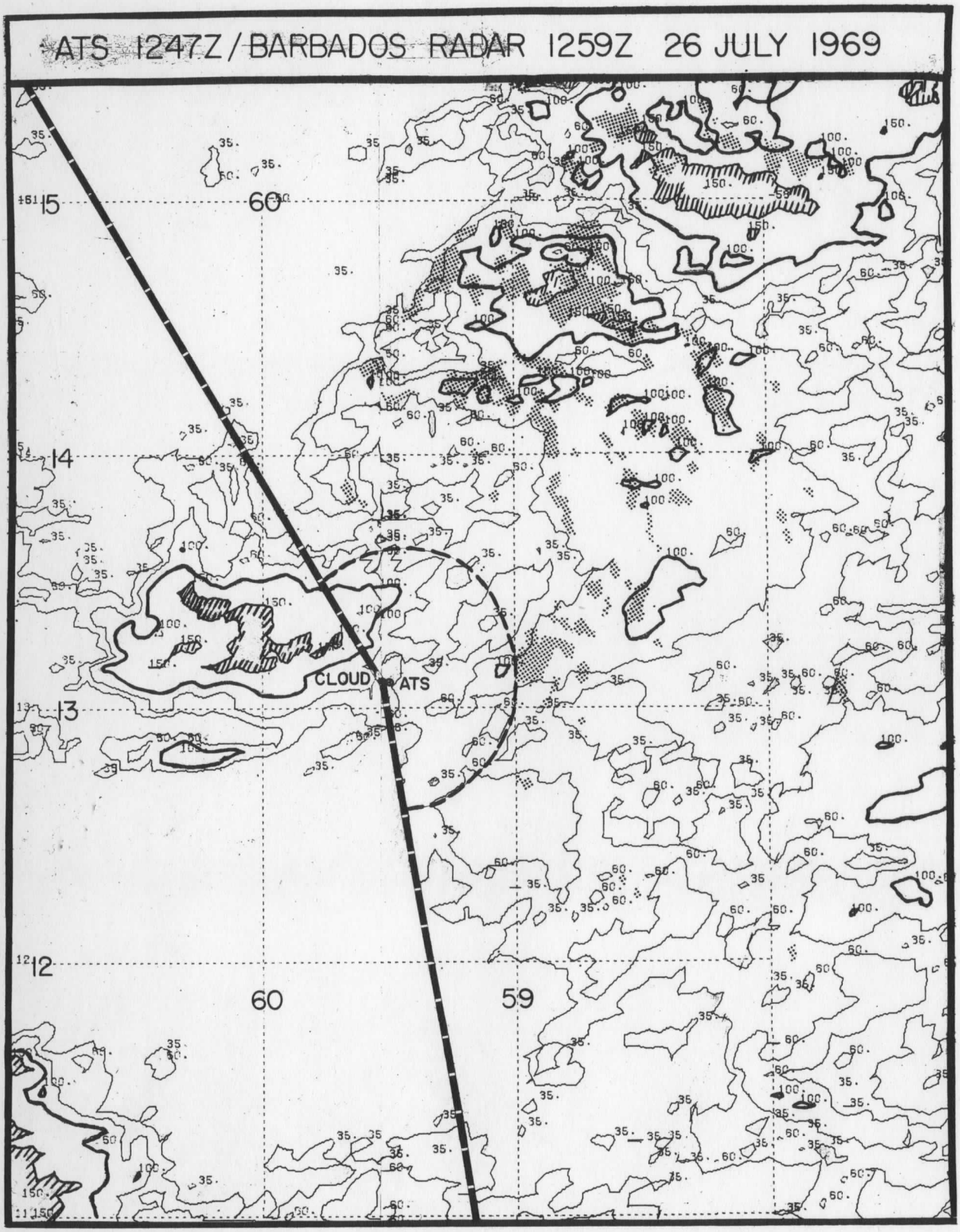

Figure 19. As for Figure 16, except Barbados radar.

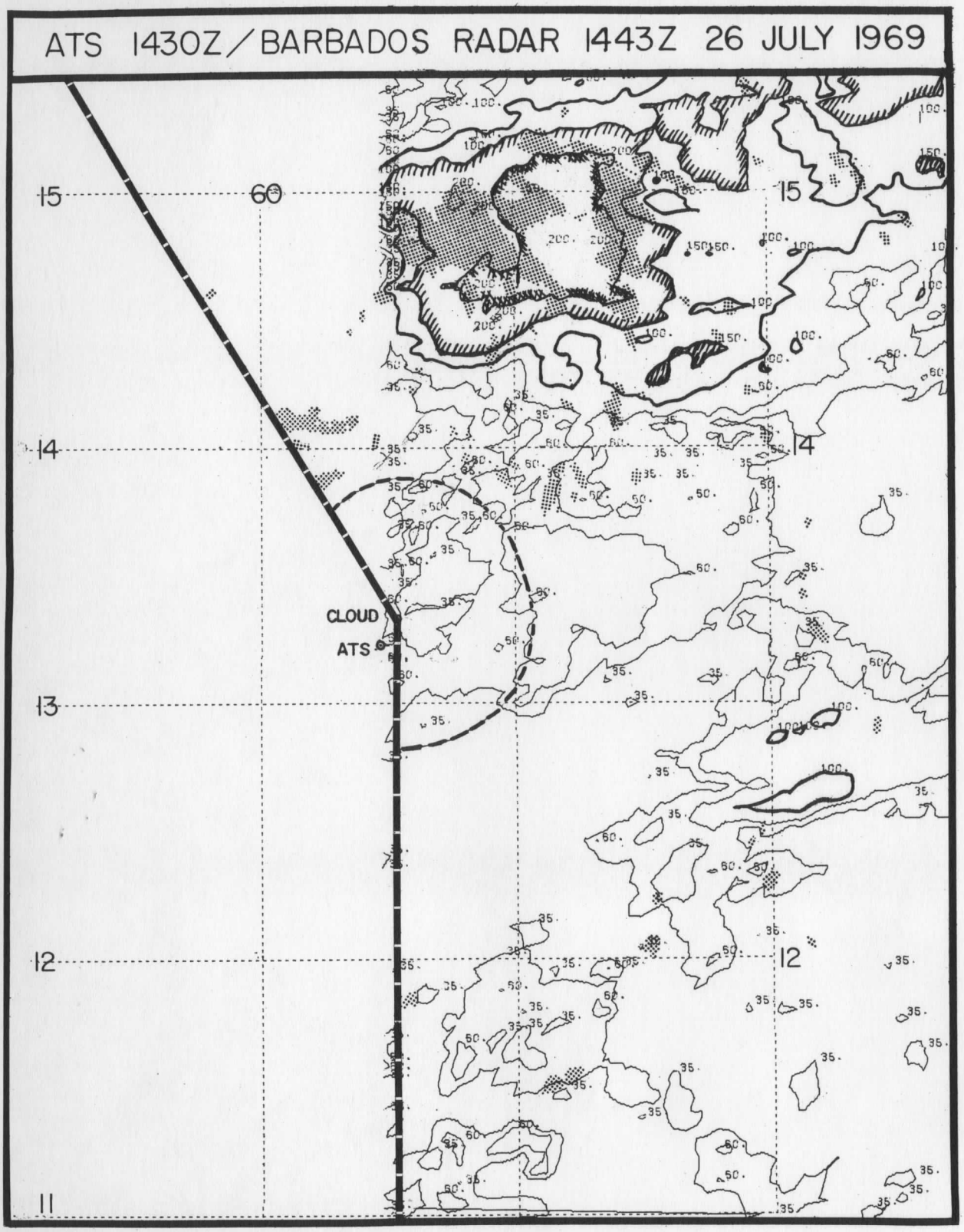

Figure 20. As for Figure 16, except Barbados radar.

The Discoverer series on 27 July were troublesome, apparently because dissipation of a cluster over and north of the ship left much cloud debris. Echoes and brighter clouds agreed quite well at 1249/1259Z (0913/0923 local), especially large echoes and the 100 contour ringing the radar on western and southern sides (Figure 21). At 1507/1516Z (1131/1140 local) the large echoes had disappeared (Figure 22) and in spite of increasing sun angle the 150 and 100 closed contours had vanished or drastically shrank. Although point to point agreement between small echoes remaining and pockets of bright cloud was poor, the larger scale patterns were consistent.

The Barbados radar at 1249/1302Z (0913/0926 local) on 27 July was scanning the backside of the disturbance that moved north of the island the day before (Figure 23). Allowing for a five minute time difference, coincidence between small echo and small cloud patterns is excellent. There are too few large echoes for extensive comparison, but it is noteworthy that within the contoured region the large echoes on the edge of the radar image to the north-northwest of the radar fall within 150 and 100 contours.

Agreement has improved in picture comparisons at 1353/1402Z (1017/1026 local). Patterns of radar and ATS are very close (Figure 24). This agreement is maintained in the next picture pair (Figure 25), at 1507/1515 local). Westward movement of the disturbed area has left only four small peaks of radiance over 100 digital counts; each of these enclosed or intercepted moderately large echoes.

Although the sample is limited in time and space, the consistent agreement found between very bright areas and large echoes in a variety of synoptic situations is clear and convincing evidence that ATS images can be used to isolate deep convection.

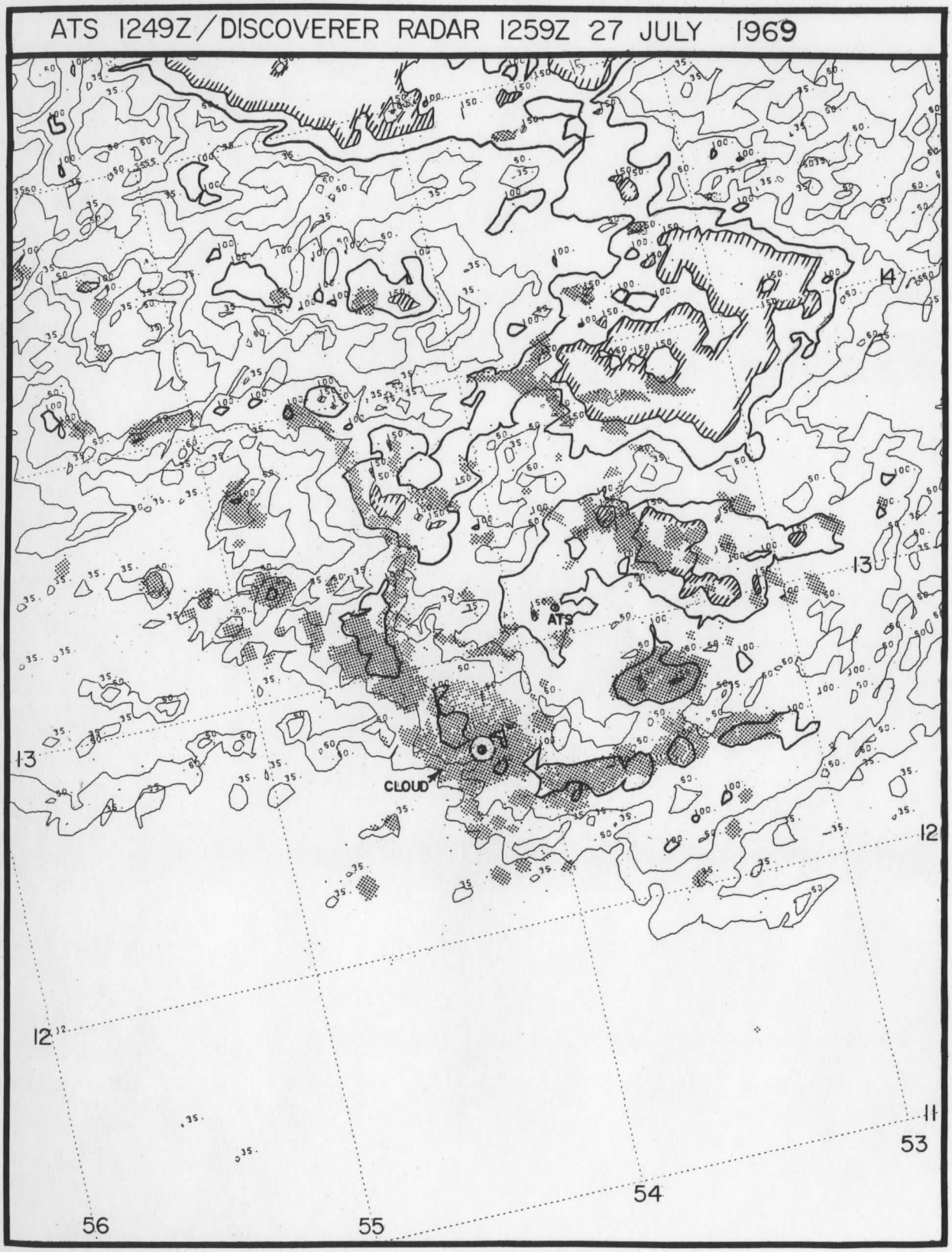

Figure 21. As for Figure 16.

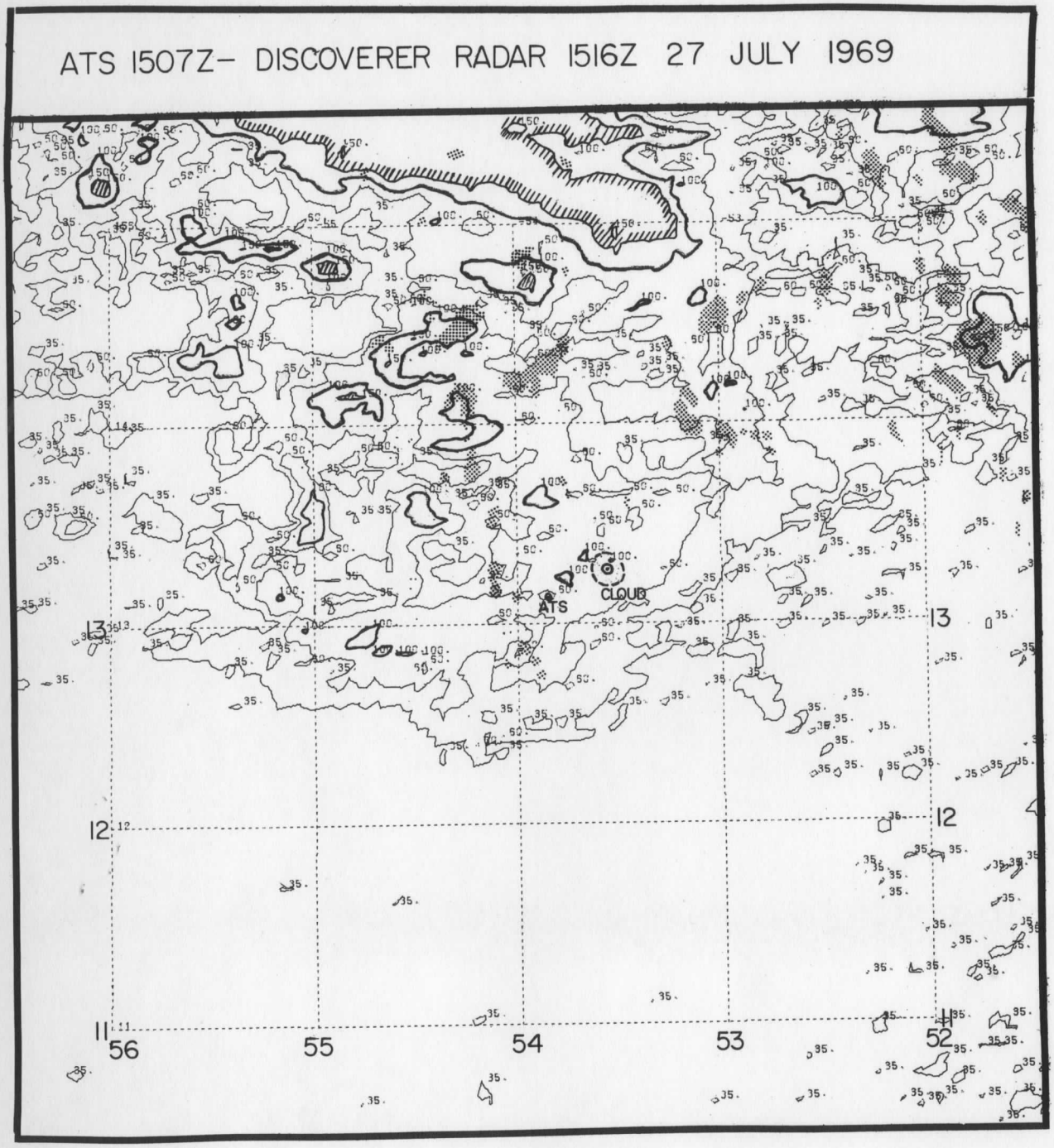

Figure 22. As for Figure 16.

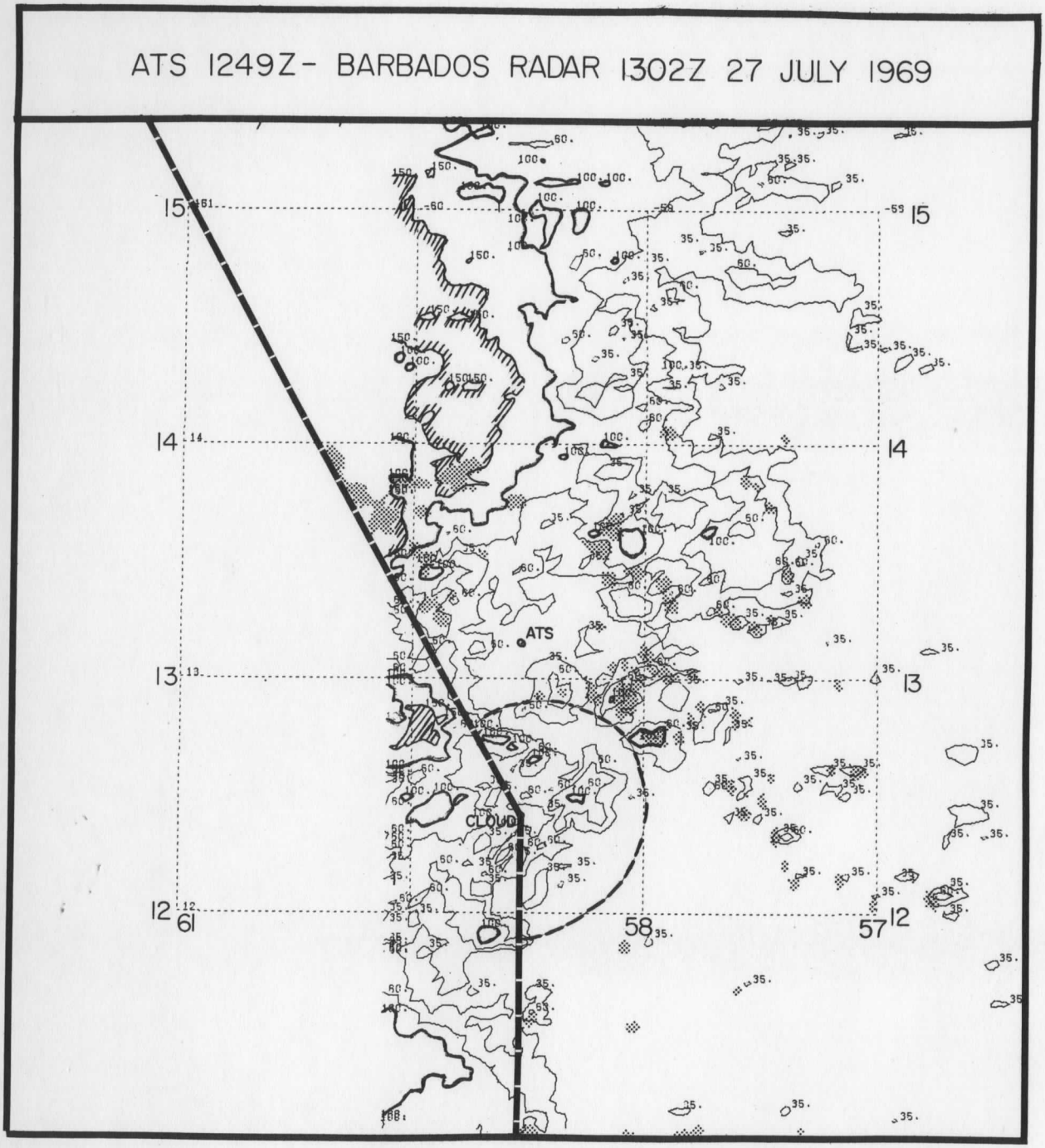

Figure 23. As for Figure 16, except Barbados radar.

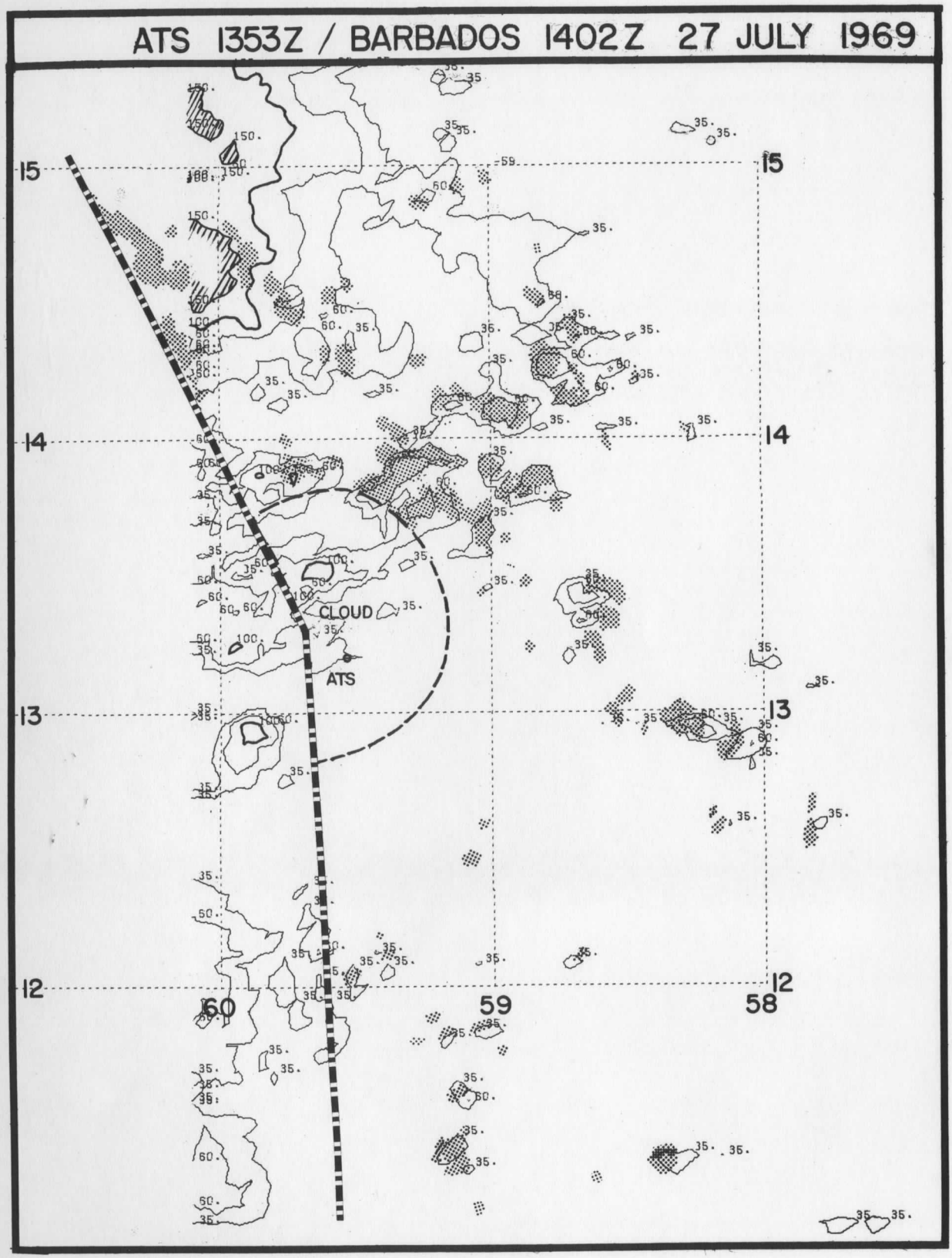

Figure 24. As for Figure 16, except Barbados radar.

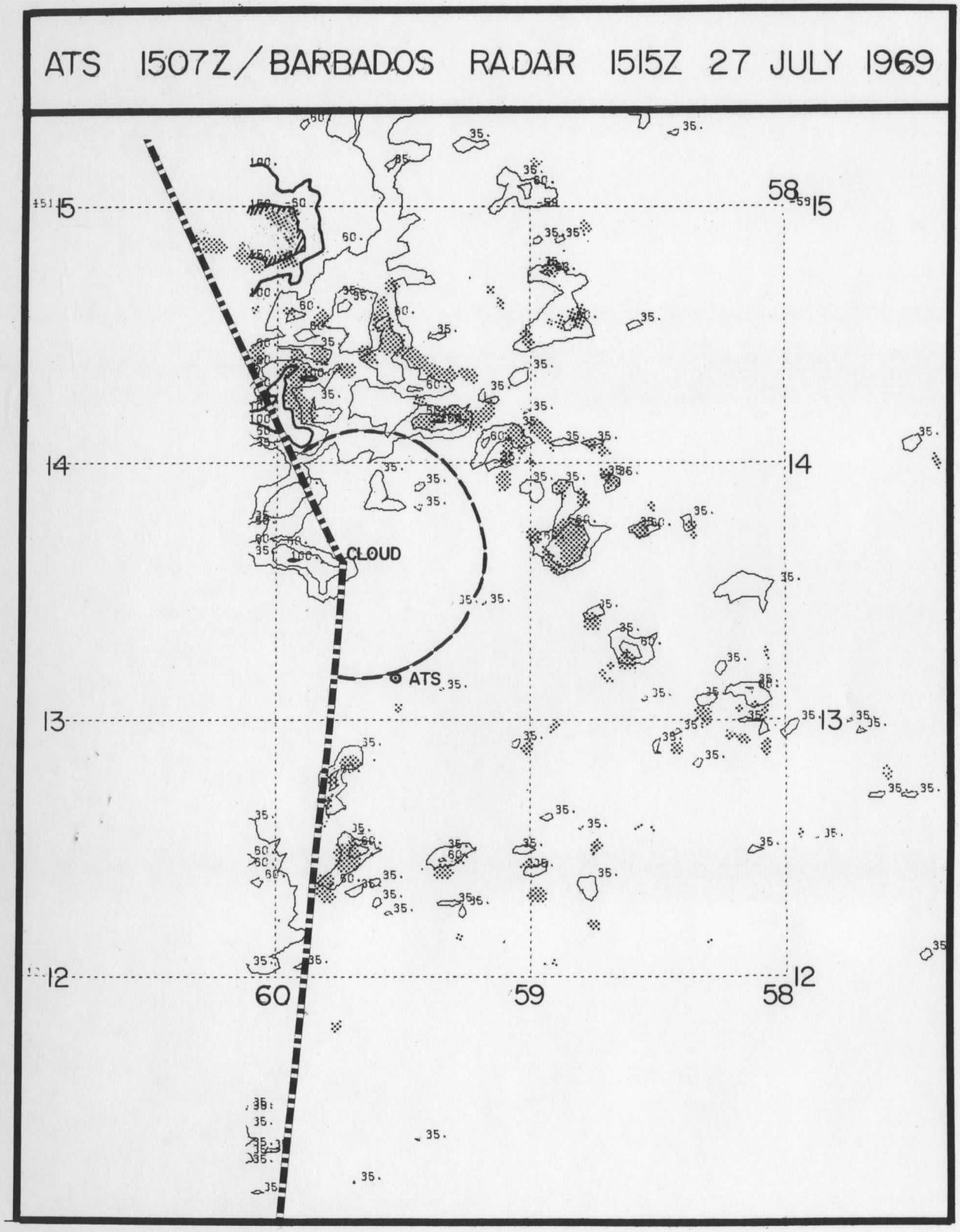

Figure 25. As for Figure 16, except Barbados radar.

Case Studies

Five days having extended series of ATS-III pictures were selected for intensive study of convective activity. From these five picture sequences eight cloud clusters were analyzed by means of time series tracings of core and cloud areas. Clusters were positioned along the time line by reference to some geographic feature appearing in all the pictures, or to a persisting feature of the cluster. Rotational orientation was fixed by reference to two land marks or by maintaining a constant angle between the time line and scan lines.

From these time series a number of core statistics were derived, among them core number, size, lifetimes, movement, and banding. Shapes, spacing, location, new growth, and diffluence/confluence were noted where appropriate. Geographic positioning resulted in large variation from picture to picture; hence an excessive noise component on velocities of cores. This was reduced by applying a three step smoothing to all velocities. Lifetime statistics are limited by the three to four hour interval over which the cosine law change of radiation is relatively small. Length of life was measured by counting the pictures in which a core appeared, making appropriate allowances where picture interval was variable.

Ansel

For ease of identification, clusters are given names. A photographic time series of the first, Ansel, (Figure 26) shows the appearance, evolution, and disappearance of cores as the sun approaches and passes local noon. Comparison with the time series tracing (Figure 27) shows the correspondence between tracing and original enhanced picture.

Ansel was a small cluster which appeared over the central Caribbean on 25 September 1970. During the picture interval it had a maximum of 12 cores

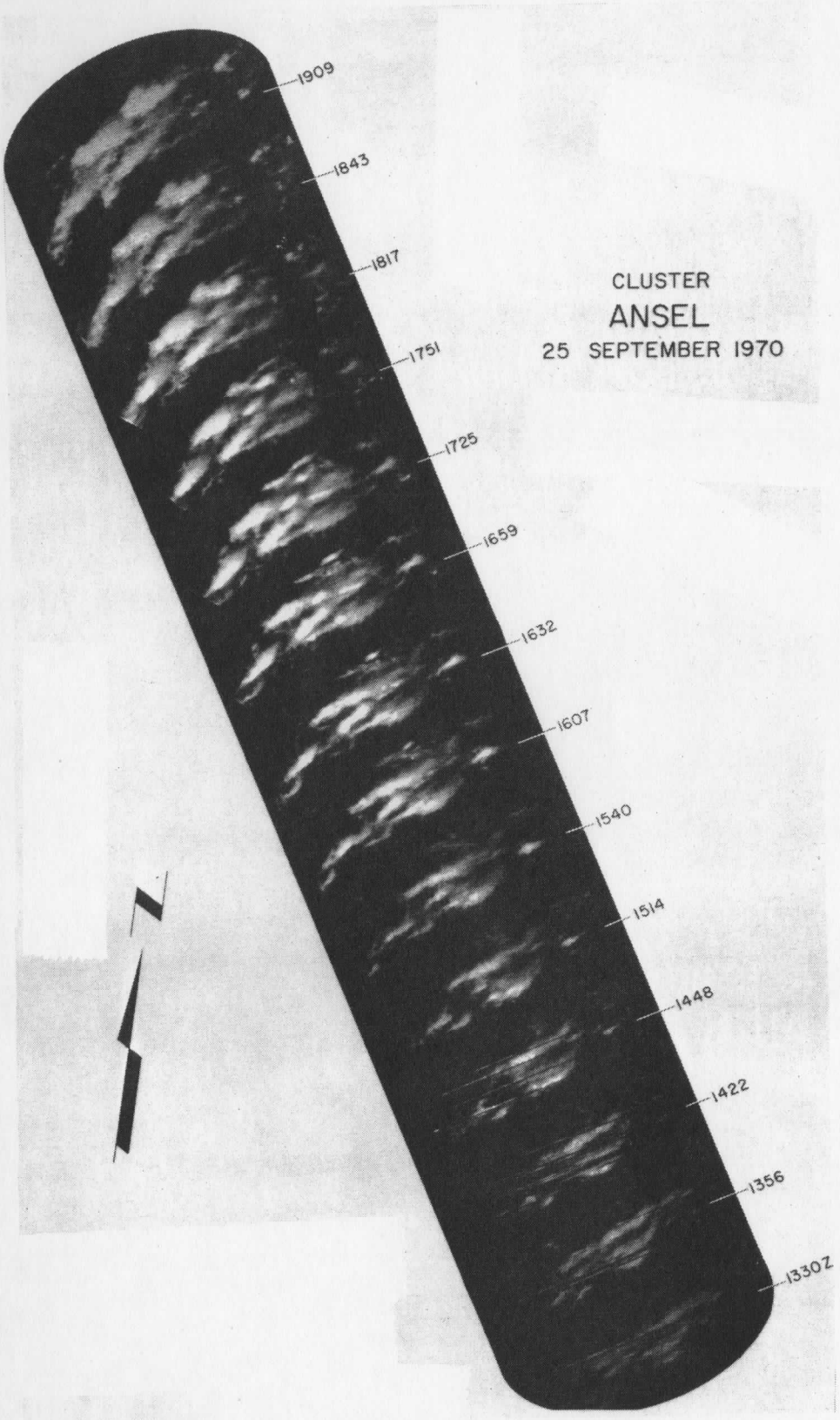

Figure 26. Time series of photographs of cloud cluster Ansel for 25 Sept., 1970. Picture times are Greenwich.

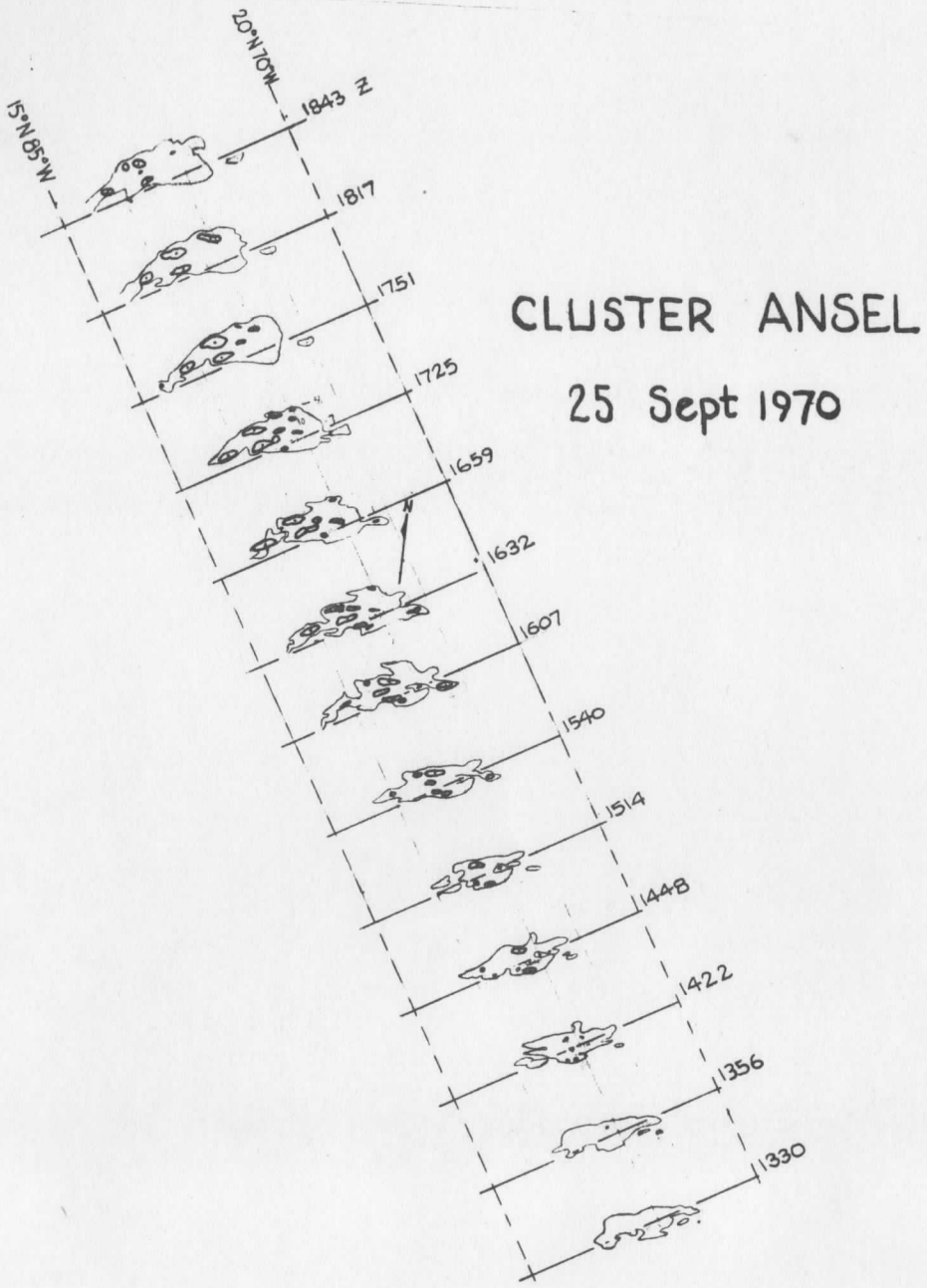

Figure 27. Time series of tracings of core and cluster areas for Ansel on 25 September 1970.

(Figure 28). Rapid growth of new cores from 1600Z to 1800Z resulted in total core area increase well beyond local noon at 1710Z. This increase in convective activity was accompanied by a doubling of the cluster area.

Cores tended to be elongated in the east-west direction, approximately parallel to the long axis of the cluster. Their spacing was fairly uniform, except for one core which formed off the eastern end of the cluster. An alignment of cores into east-west bands is evident; there was at the same time a suggestion of banding in a northeast-southwest direction. Spacing of bands was 80 km and about 130 km, respectively.

Core lifetimes fell into two groups - less than 90 minutes, and two to four or more hours. In general large cores lived longer than small cores.

The cluster reference point, a persistent hole in the clouds, was nearly stationary through the picture series; therefore displacements measured from it are approximately equivalent to true ground movement. In respect to the time line coordinate system cores moved down axis and leftward early in their lives, then rightward at diminished speed as they decayed. This is equivalent to initial westward movement of about 10 m/sec becoming eastward at about 5 m/sec.

Determination of movements was complicated by merger of existing cores with new cores forming to the west. Cluster movement, which was measured by reference to landmarks as WNW at 7 m/sec over the picture series, was accomplished by the individual movement of clouds plus the formation of a new band on the north side of the cluster and the formation of new cells on the west ends of existing bands as the southern most band and easternmost cells dissipated. The net effect was for the cluster to be displaced more rapidly than individual cores.

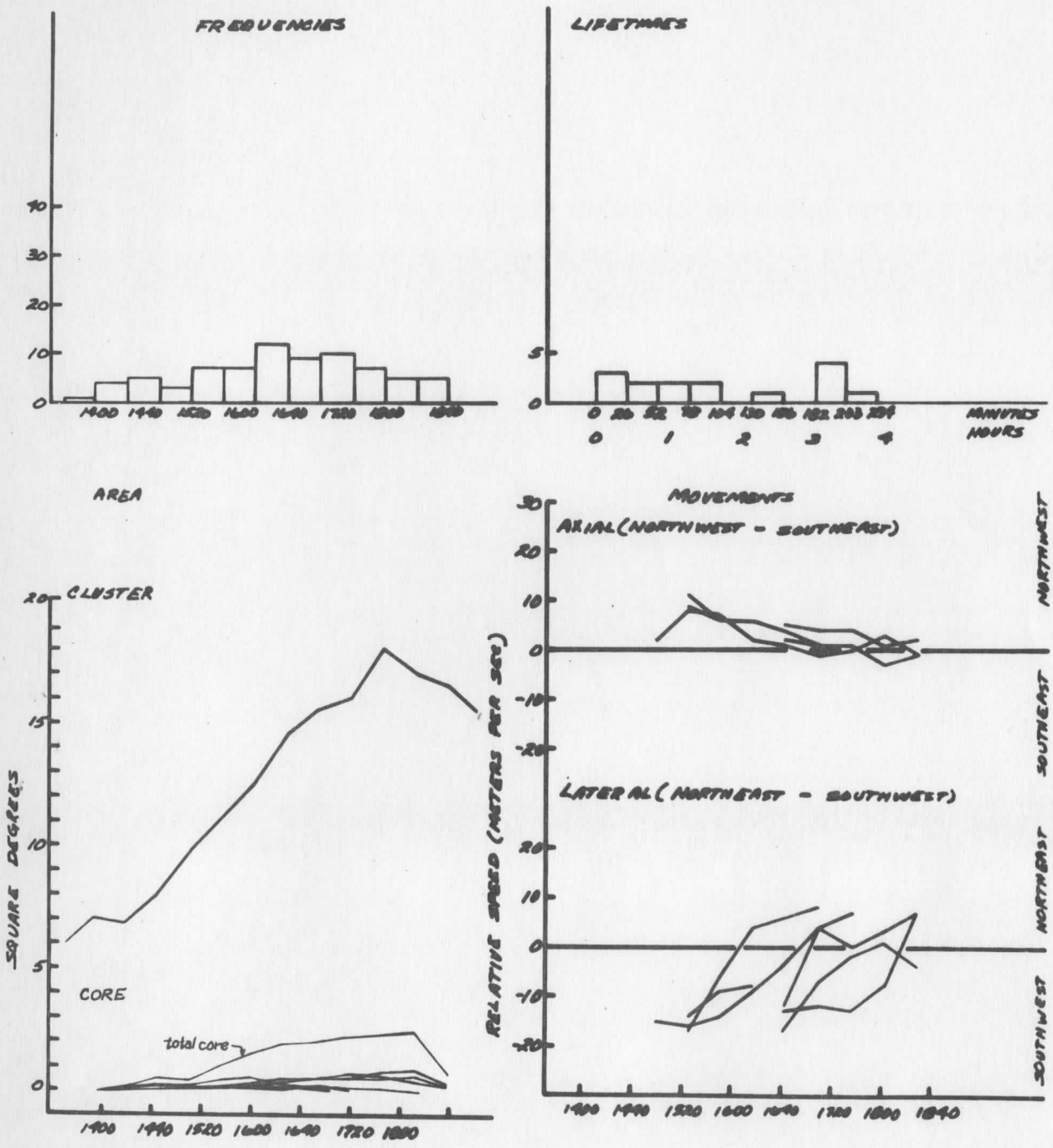

Figure 28. Characteristics of cores for cluster Ansel; statistics derived from the 25 September 1970 time series.

The organization of cores, together with the patterns of core and band growth and dissipation is suggestive of the interference pattern formed by two nonparallel propagating wave trains.

Of particular interest is the core which developed just east of Ansel. It appeared first in picture 1330 as a cloud just over the threshhold of camera resolution. Rapid growth occurred over the next two hours. By 1540Z a core was visible, and by 1607Z this cloud had merged with the main cluster cloud mass. Core area began to decrease in picture 1632. The core disappeared between pictures 1659 and 1725, during the time when the sun was at its zenith. Picture 1725 shows the remaining cloud breaking away from Ansel. Over the next three pictures this cloud steadily decreased in area as it moved away.

Plots of velocity of the cloud and its core show an initial westward movement at 10 to 12 m/sec veering to northwestward at 8 to 10 m/sec by the time of core appearance. Forward movement decreased to 3 to 5 m/sec during the short interval of core prominence, then increased with continued veering as the core disappeared. During the last three pictures of the series cloud movement was eastnortheast at about 20 m/sec.

The satellite has recorded, with unusual clarity and completeness, the life cycle of a giant cb or small thunderstorm complex. Movement of the cloud can be understood in terms of growth and decay in a shearing wind field - an easterly current below an upper level west to southwest flow. A three stage cycle of growth is suggested: production of an aggregation of small cumulus clouds through boundary layer convergence, and movement of these clouds westward in the ambient flow; deep convection extending from boundary layer to upper troposphere, and exchange of momentum resulting in motion intermediate between lower and upper level wind fields: then

dissipation of middle and low clouds as convection ceases, and movement of the more persistent cirrus plume with the upper level winds. Of special significance is the coincidence of the bright spot with the period of large change in cloud movement. It suggests that in this enhanced picture series bright spots did closely correspond with deep convection.

Greta

Cluster Greta is named after the tropical storm into which it developed on the day following the time series from ATS. This system over a three week period traversed the Atlantic and meandered across the Gulf of Mexico before breaking up over the mountains of Mexico (Simpson and Pelissier, 1971). On 25 September 1970, the day of the ATS picture series (Figure 29), Greta was located east and north of Hispaniola.

During this picture series Greta had a maximum of 27 cores (Figure 30).* Individual cores had areas of 0.1 to 0.5 deg^2, with a few areas up to 1.5 deg^2. Most cores were elliptical in shape with the long axes east-west in the north, tending to northwest-southeast in the south. Cores were concentrated in four main groups within the primary cloud mass; however, spacing was fairly regular in the cloud band which formed to the northwest.

Allowing for the bias due to noise the distribution of lifetimes shows an approximately hyperbolic decline in lifetime frequency out to about 4 hours. To a limited extent the dominant effect of sun angle change is compensated in the distribution which is limited to lifetimes of cores first appearing in pictures 1448 and 1514. This curve suggests that the majority of cores had lifetimes less than 3 hours.

---

*Statistics describing this cluster are impaired by noise on the ATS signal in pictures up to 1514Z. This noise produced an artificial peak in core numbers and area at 1448Z, and an inflated peak in lifetimes at 26 minutes.

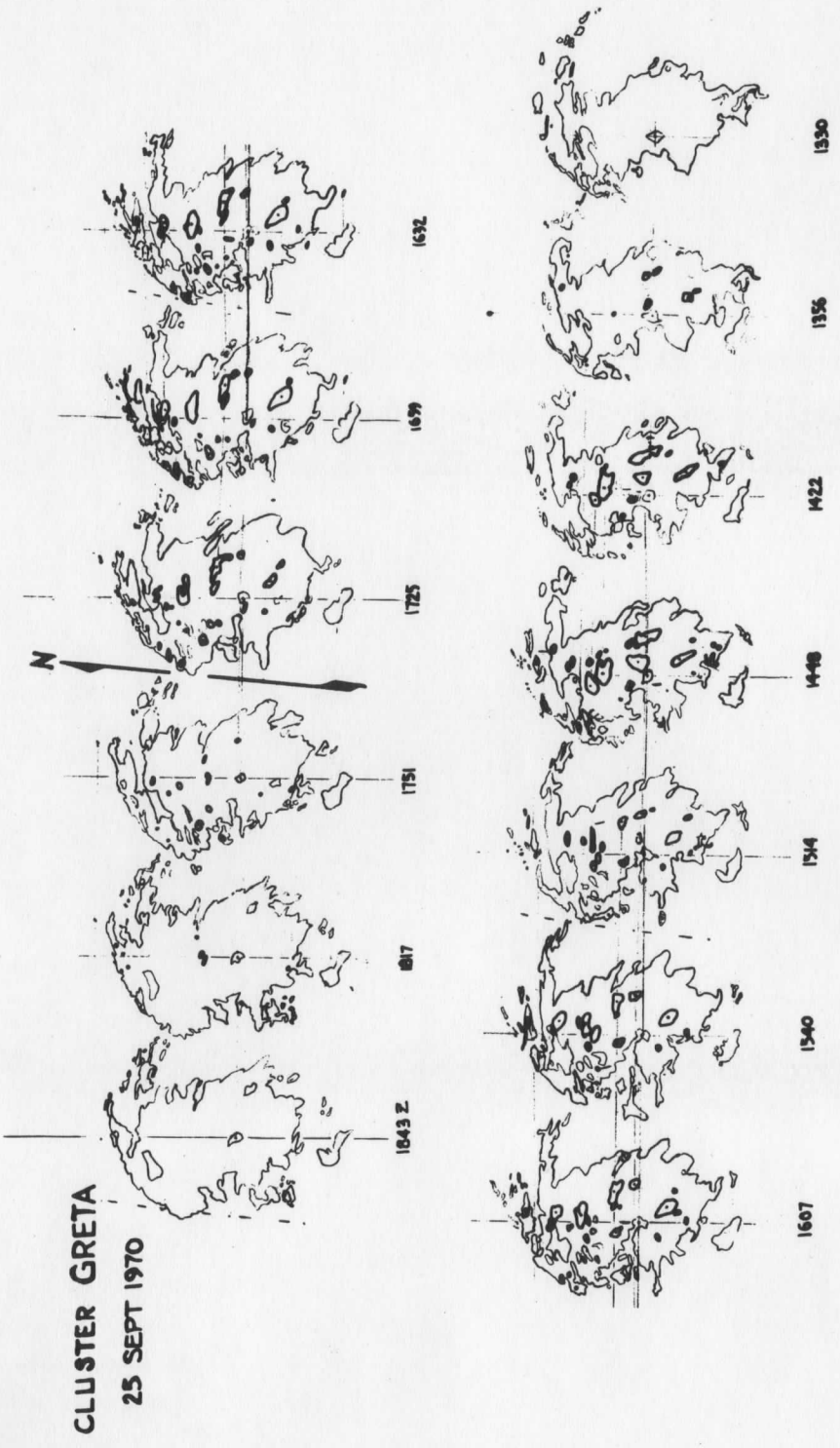

Figure 29. Time series of tracings of core and cluster areas for Greta, 25 September 1970

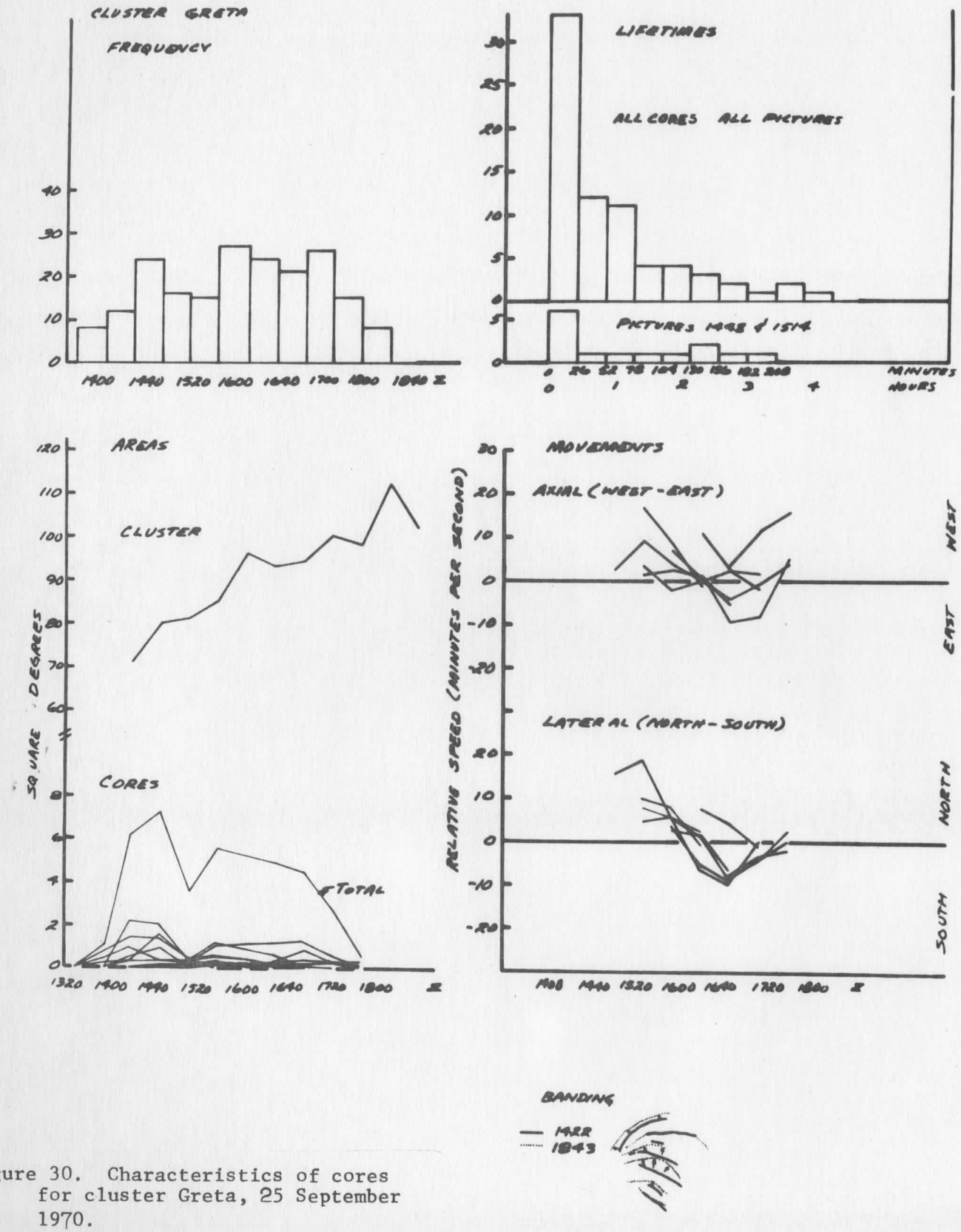

Figure 30. Characteristics of cores for cluster Greta, 25 September 1970.

Large variations in positioning the reference point mask movements, but the averages (corrected in two pictures for misplaced reference point) of several cores evolving between the first and last pictures of the sequence show that movement of cores was initially northwestward relative to the reference point, then became southeastward. Since the reference point itself was moving northnorthwest at roughly 8 m/sec, with few exceptions true core movements were predominantly northwestward at decreasing speeds through their lifetimes. This is consistent with the model of deep convective evolution in a shearing layer described previously; the shear in Greta was between a southeast to east boundary layer flow and an anticyclonically curving southwest to northwest flow aloft.

Most of the larger cores appear to be the product of one or more mergers which occurred rather frequently. Careful examination of these cores suggests that some of the original smaller cores retained their identity through several pictures in spite of close proximity to other cores.

Banding occurred in east-west lines, which arced from southwest to southeast in the north, and west to southeast in the south. Curvature was especially pronounced toward the north. Spacing of the lines varied from about 160 km at the western ends to about 360 km at the eastern ends. The central bands moved north-northwestward at 10 to 15 m/sec; movement of the northwestern band was about 10 m/sec toward the northwest; the southernmost band remained almost stationary. Growth of cloud at the western ends resulted in a general westward displacement of the bands.

The pattern of cirrus plumes (Figure 31) was strongly diffluent, suggesting extensive upper level divergence through the entire picture sequence. This also was a period of pronounced convective activity, and immediately preceded designation of the system as a tropical storm.

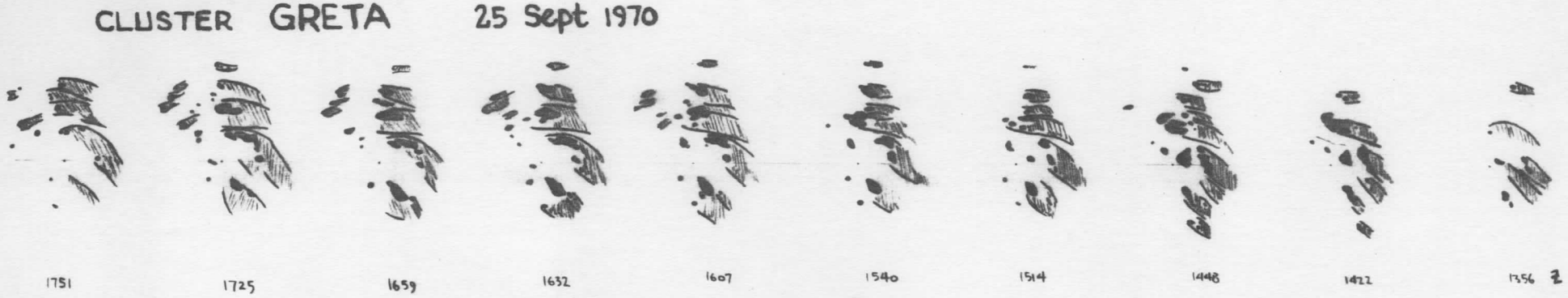

Figure 31. Cores and cirrus plumes traced from the complete day picture series for cluster Greta 25 September 1970

Dorothy

Like Greta, cluster Dorothy was a named disturbance having origins over Africa. Dorothy reached tropical storm intensity the day before the ATS III picture sequence for 20 August 1970 which is examined here (Figure 32). She contained two primary concentrations of cloud cores, one to the east of the Leeward and Windward Islands, and one west of the Windward Islands. A third group of cores, which formed over South America, is included for comparative purposes. These cores show up first in picture 1520 at about 1100 local time. They evidently represent "popcorn cumulonimbi" - convective clouds triggered by solar heating of the surface - which are dominant among cloud systems over tropical South America (Report of the first session of the Study Group on Tropical Disturbances, contained in GARP Publications Series No. 4, 1970).

The maximum number of cores observed in Dorothy was 29 (Figure 33). These were about equally distributed between eastern and western parts. Four cores, three east and one west, grew to very large size, 2 to 4 deg^2. Central cores in the eastern group tended to be round; to the northeast of the center and on the western end cores were elongated east and west. Spacing was irregular. Within both of the primary concentrations many cores were side by side; others developed in isolation.

Most cores were short lived; however there was a tendency for frequency peaks around 2 hours and 3 to 3.5 hours. This pattern was repeated in the lifetime distribution of all cores first appearing in picture 1454. Tabulations for cores over South America contained only the first and second peaks. New cores tended to form on the western sides of the primary groups. Although cluster area became somewhat ambiguous as connecting cloud formed

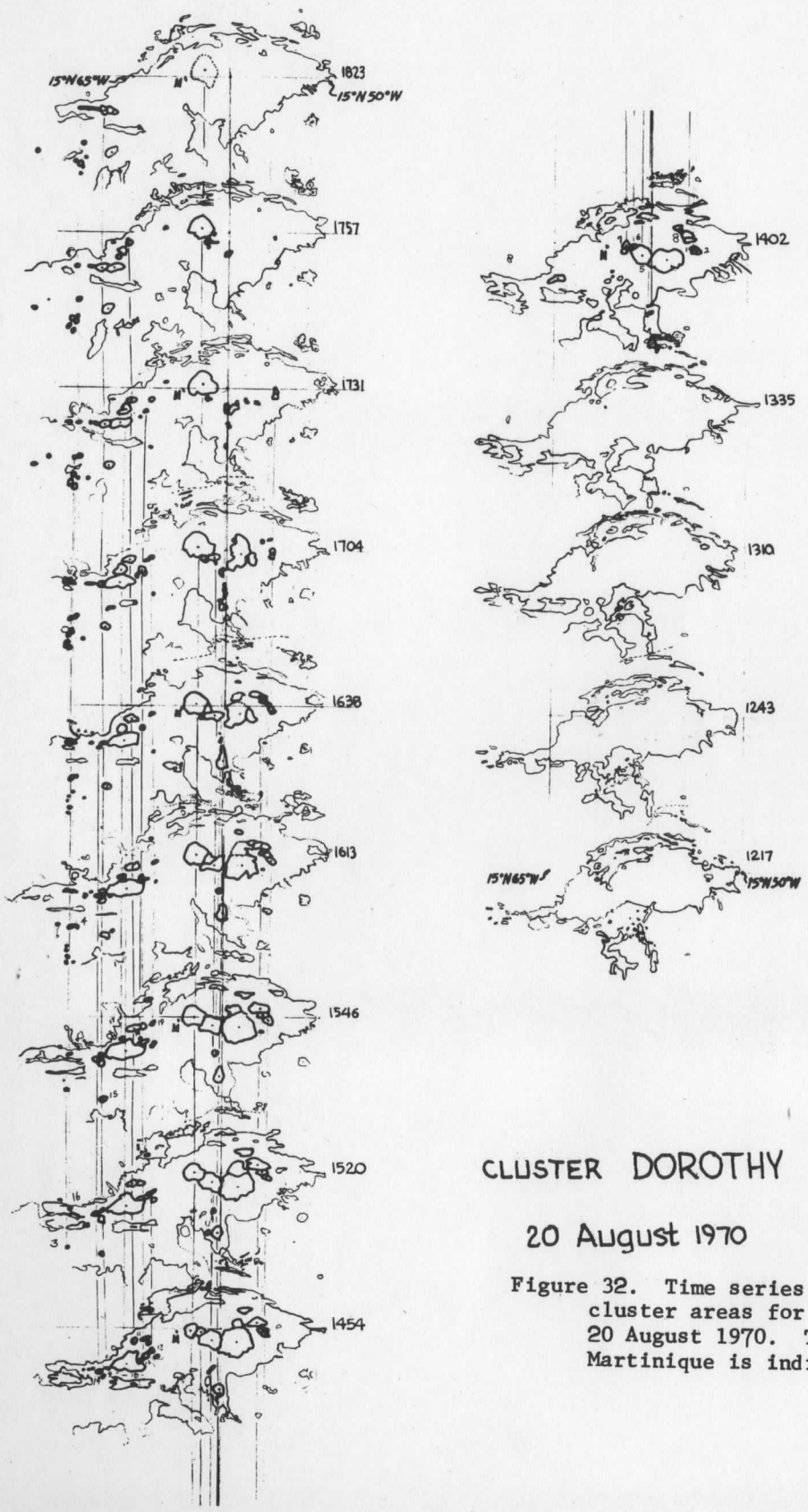

CLUSTER DOROTHY

20 August 1970

Figure 32. Time series of core and cluster areas for cluster Dorothy, 20 August 1970. The Island of Martinique is indicated by an "M".

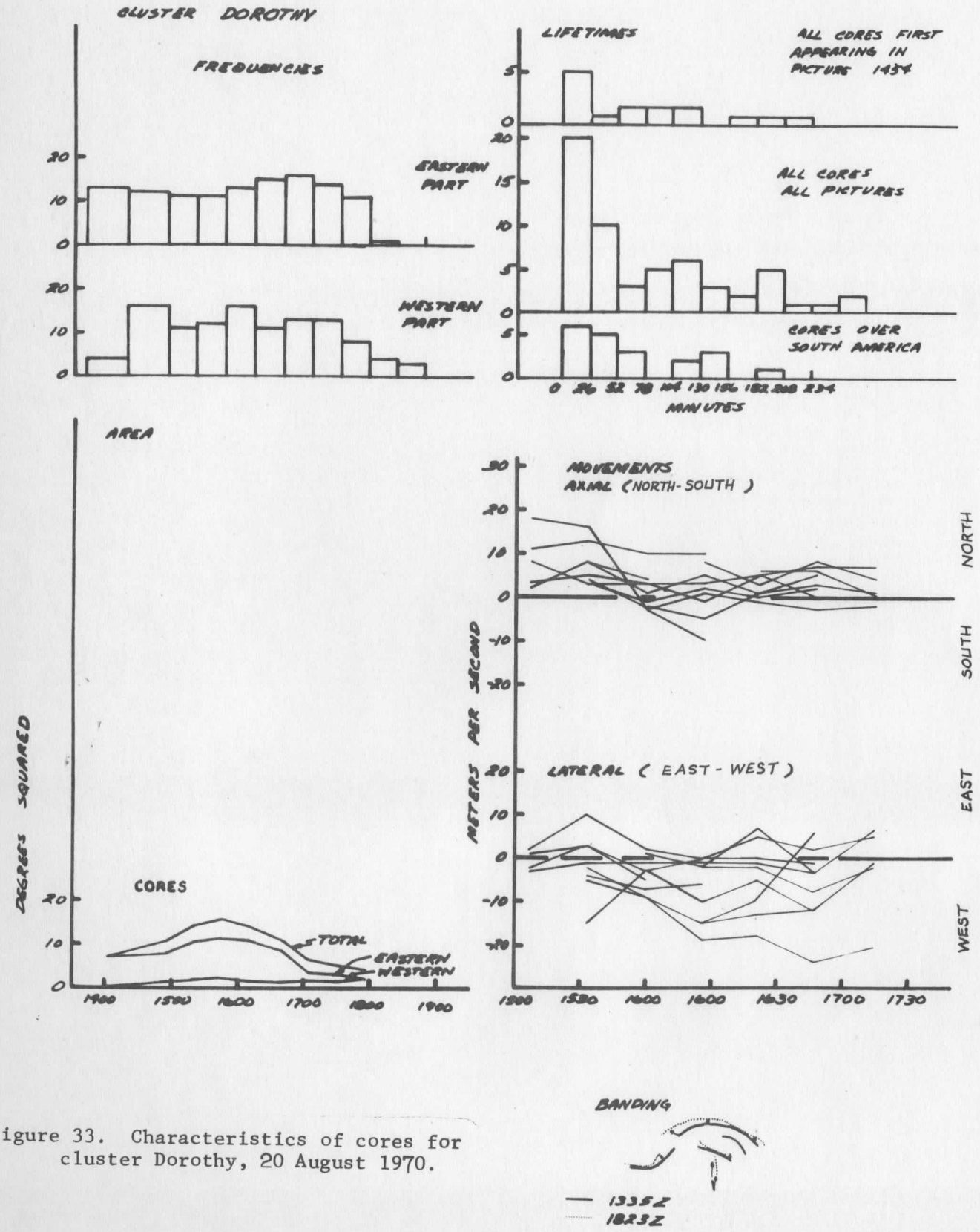

Figure 33. Characteristics of cores for cluster Dorothy, 20 August 1970.

over South America late in sequence, cloud around the eastern and western core groups virtually doubled in area over the period.

Banding formed a complex pattern. There appeared to be four major bands of cores, plus one long band of low and middle cloud which arched from west to east to the north of the eastern group. This band moved north and northwestward at 5 to 10 m/sec. The westernmost band moved northwestward at similar speeds. Of the other three only the southernmost showed appreciable displacement, a movement northward along its axis at 10 to 12 m/sec. Since low level cloud motions in its vicinity were near zero and plume orientation suggested northerly upper level winds, this motion apparently was accomplished mainly by propagation.

Within a few hours of this picture sequence tropical storm Dorothy crossed the Antilles chain. Damage was heaviest on the island of Martinique, where sustained winds of 30 m/sec and gusts to 44 m/sec were recorded. Fifty lives were lost in floods and landslides caused by heavy rain (Simpson and Pelissier, 1971). In picture 1402Z Martinique lay some 80 km west of a small core which underwent explosive growth over the next three hours. By 1731Z, the growth of this core together with shrinkage or complete disappearance of other cores in the group brought it to complete dominance. In size, persistence, and intensity this core was exceptional. Its proximity to Martinique near the time of the disaster is indicative of a contributing, if not primary, role in the generation of the gales and torrential rains accompanying storm Dorothy's passage.

Delbert

On 21 July 1969 ATS III observed three active clusters near the coast of West Africa (Figure 34). The easternmost of these, named Delbert, was

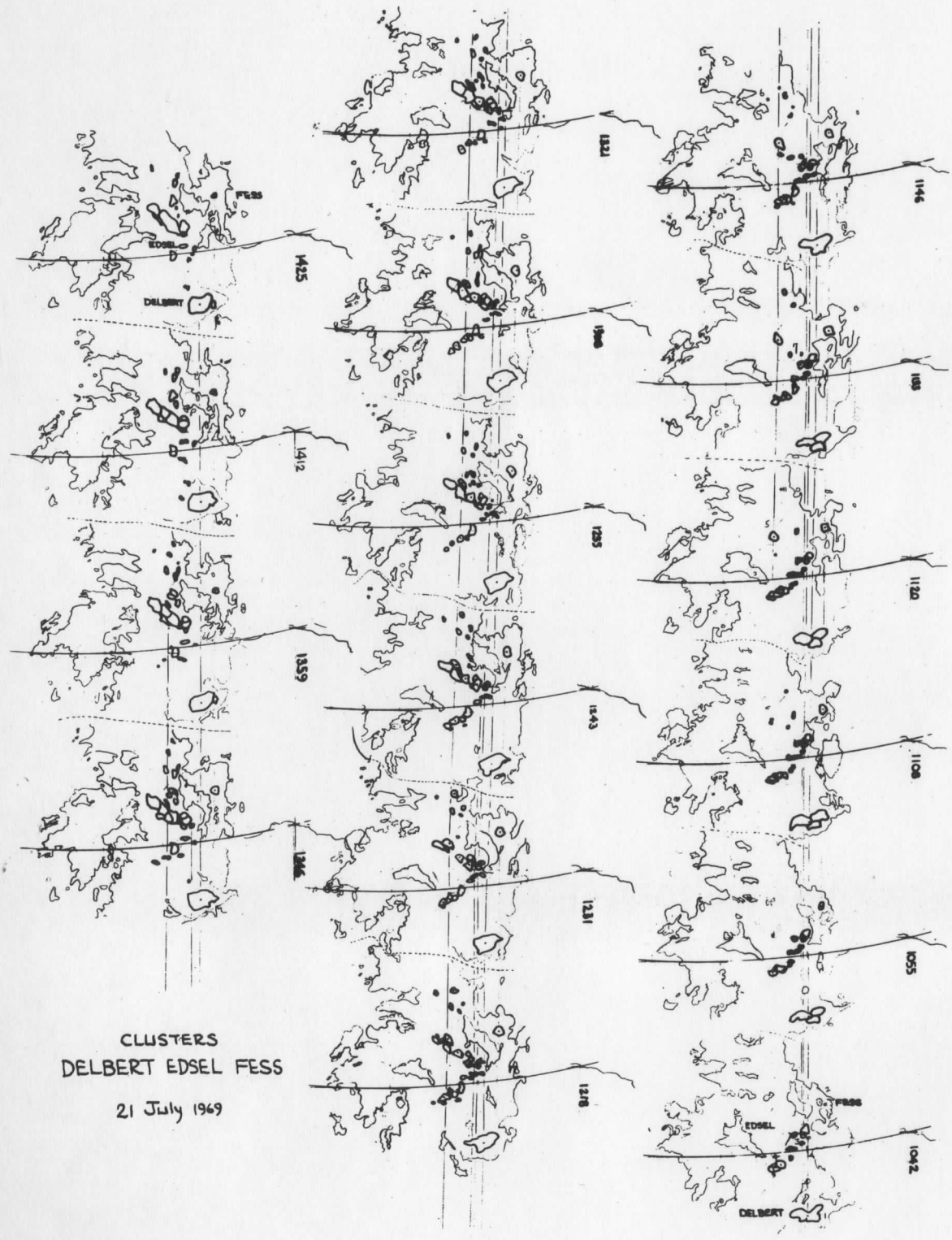

Figure 34. Time series of core and cluster areas for clusters Delbert, Edsel, and Fess, 21 July 1969.

typical of a class of squall-like disturbances that propagate across West Africa below the Sahara Desert.

Three cores visible in the first five pictures became one giant core through dissipation of the southernmost core and merger of the eastern core with the northern core. This core, 4.5 to 5 deg^2 in area, persisted through the rest of the sequence. The few cores which appeared late in the series were small and short lived. Through the entire series the large core maintained a north-south orientation, with long axis 1.5 to 2 times the length of the short axis. Displacement over the period was westerly at 5 to 10 m/sec.

Fess

Cluster Fess was like Delbert in its domination by a single core (Figure 34). This core had an area of 0.5 to 1 deg^2, and was nearly circular in shape. It was located in the eastern part of the cluster, well separated from other cores. Like the core in Delbert it persisted throughout the 4 hour picture series. Cluster area doubled during this time.

The core was located on the apex of a westward moving wave-like band, which late in the series developed an extension west from the wave crest. Core movement averaged over the entire period was westnorthwest at about 13 m/sec.

Edsel

Between Delbert and Fess was a rather poorly defined cluster which has been christened Edsel. Cores within Edsel formed three groups (Figure 34). The eastern group stretched northwest-southeast along the African coast. At right angles to its northern end a second group extended southwestward. The third group consisted of cores west of the central group. All cores were located in the northern part of the main cloud mass.

Maximum core frequencies through the series were about equal for each group; however, the time of occurrence varied widely (Figure 35). Frequencies peaked well before local noon in the eastern group, around local noon in the central group, and slightly after local noon in the western group. The distribution of sizes was relatively uniform. Only in the central group late in the period did any very large cores appear. Shapes were mostly elliptical, with a tendency for the long axes to align along the bands. Within the eastern and central groups spacing was very close; it was highly variable in the western group.

Lifetimes for each of the three groups fell into three classes - less than one hour, one to 1.5 hours, and greater than two hours. Average lifetimes for each group - which are underestimates of the true lifetimes - are about 1.5 hours - for the eastern and central groups and one hour for the western group. Even if allowances are made for the early termination of the picture series, this indicates that the poorly organized western band contained short lived cores.

Banding, present in each of the core groups, was especially well-developed in the eastern and central groups. Except for the southern part of the central band, which pivoted westward, both of these bands remained quasi-stationary. As the eastern band weakened late in the period a new band appeared to be forming 200 to 250 km to the east. Proximity to the African coast, orientation, lack of movement, and patterns of growth and decay suggest that these bands might have been conditioned by sea breeze or orographic influences.

Ginger

A mid-Atlantic cluster is examined in the picture series for 21 July 1969, (Figure 36). Although this system probably contained part of cluster Edsel, for clarity it was given a new name, Ginger. Ginger was an ITCZ disturbance having two parts of sufficient distinction that they otherwise would have been

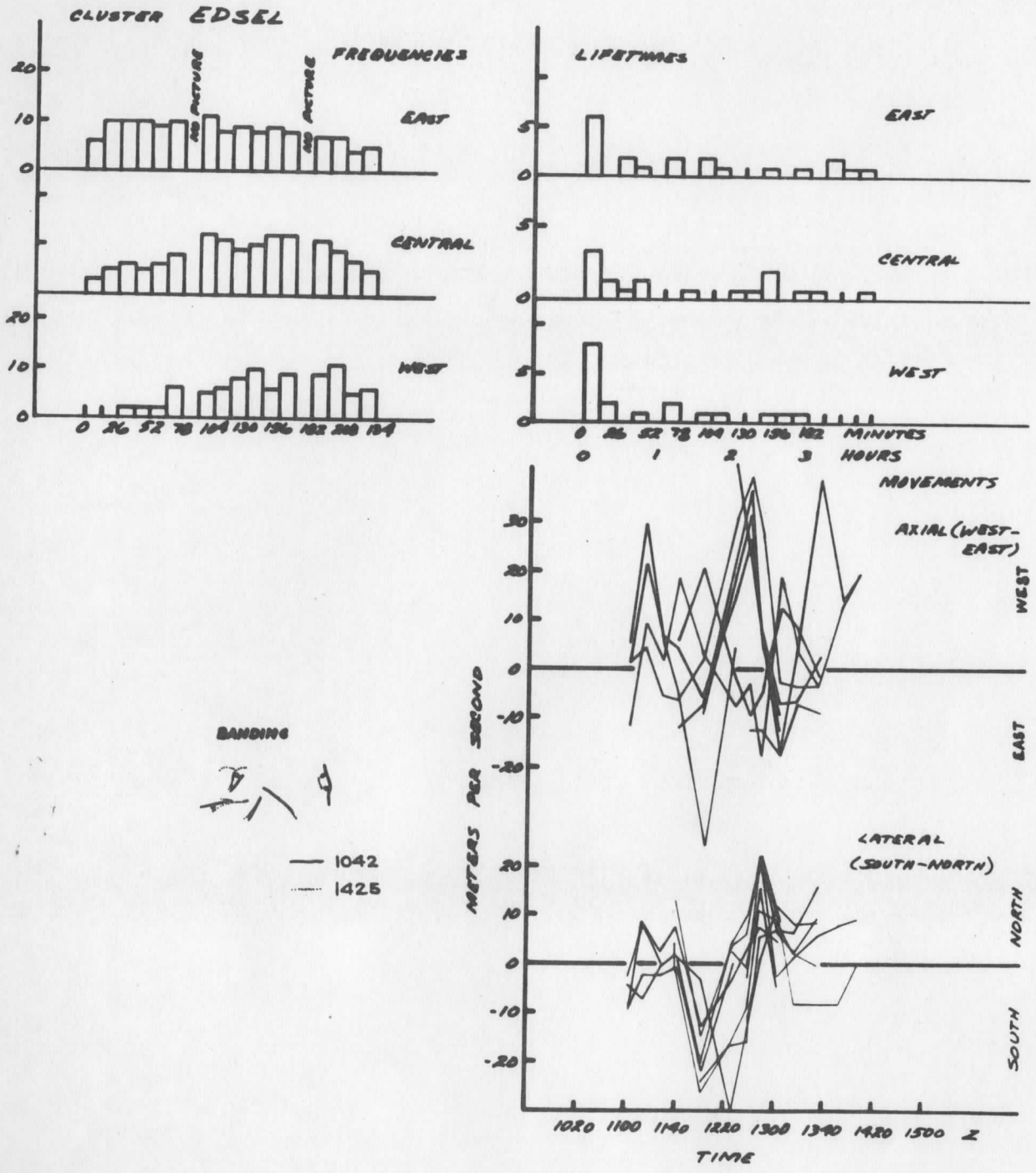

Figure 35. Core characteristics for cluster Edsel, 21 July 1969.

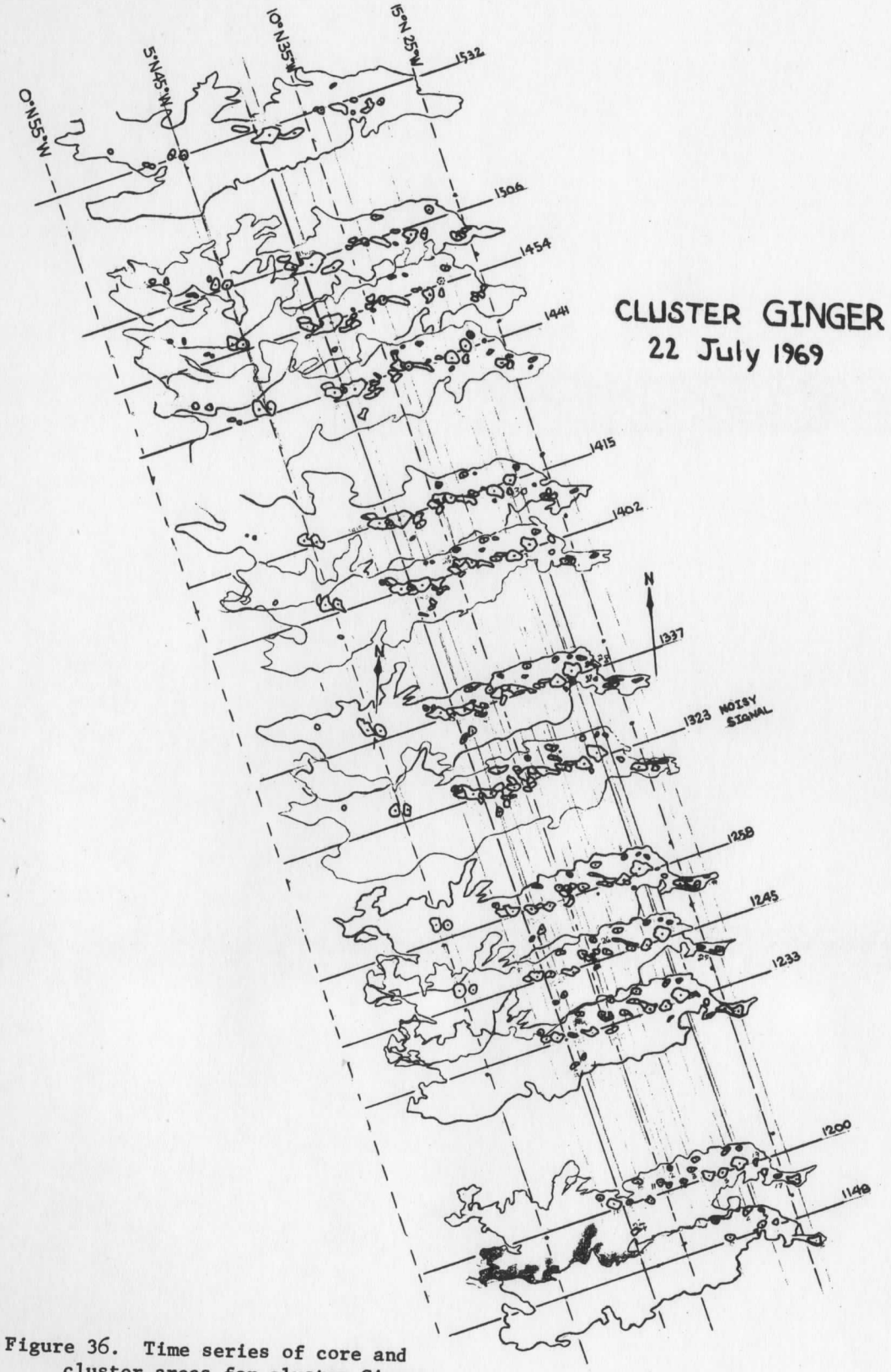

Figure 36. Time series of core and cluster areas for cluster Ginger, 22 July 1969.

considered separate clusters.

These two parts differed most substantially in number of cores, (Figure 37). The eastern group had a peak frequency exceeding 40; frequencies in the western group were at all times less than 10. Especially in the east, cores tended to be uniform in size. The largest were between 1 and 2.5 deg^2 in the area; most had areas between 0.1 and 0.4 deg^2. Spacing was very close in the central band of the eastern group. In the band along Ginger's northern edge spacing was much greater and remarkably regular - about 300 km between cores. The northern half of the cluster held most of the cores.

As for several other clusters studied there was a multimodal distribution of lifetimes, with peaks at 13, 65, 130, and roughly 175 minutes. Several cores lasted well over 3 hours.

Banding was complex. The western core group was associated with a weak spiral. Relative to the reference point, which was moving west north westward at 5 to 10 m/sec, these bands seemed to rotate cyclonically. Bands in the east formed a weak wave. Two of these bands pivoted southward around the wave crest; the band arcing across this wave simply extended itself eastward.

Anna

Cluster Anna was also a named disturbance. A ship during or shortly after the picture sequence of 27 August 1969 (Figure 38) reported winds of 21 m/sec (40 kt) "...while apparently some distance from the center" (Simpson, Sugg, and Staff, 1970). Two days later a reconnaissance plane measured winds of 31 m/sec (60 kt).

Anna had two main concentrations of cores - a tight cluster in the center of eastern vortex, and a disorganized band in the western tail. Over most of the sequence frequencies for both groups together ran between 10 and 20 (Figure 39). (The spike to 28 at 1507 is probably spurious, the result of a gain increase or anomolous processing of the picture.) Although no giant cores were present, cores

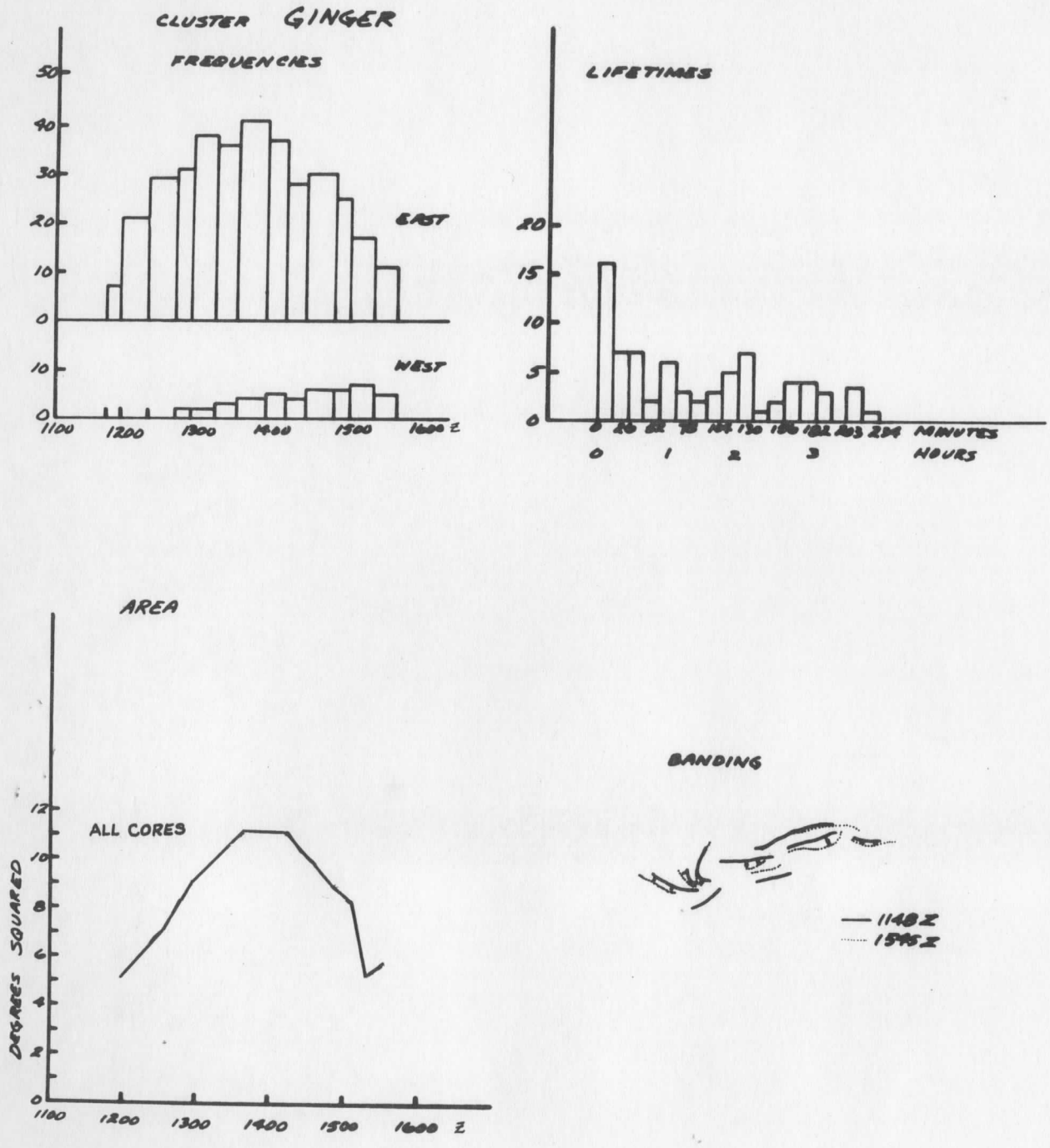

Figure 37. Core characteristics for cluster Ginger, 22 July 1969.

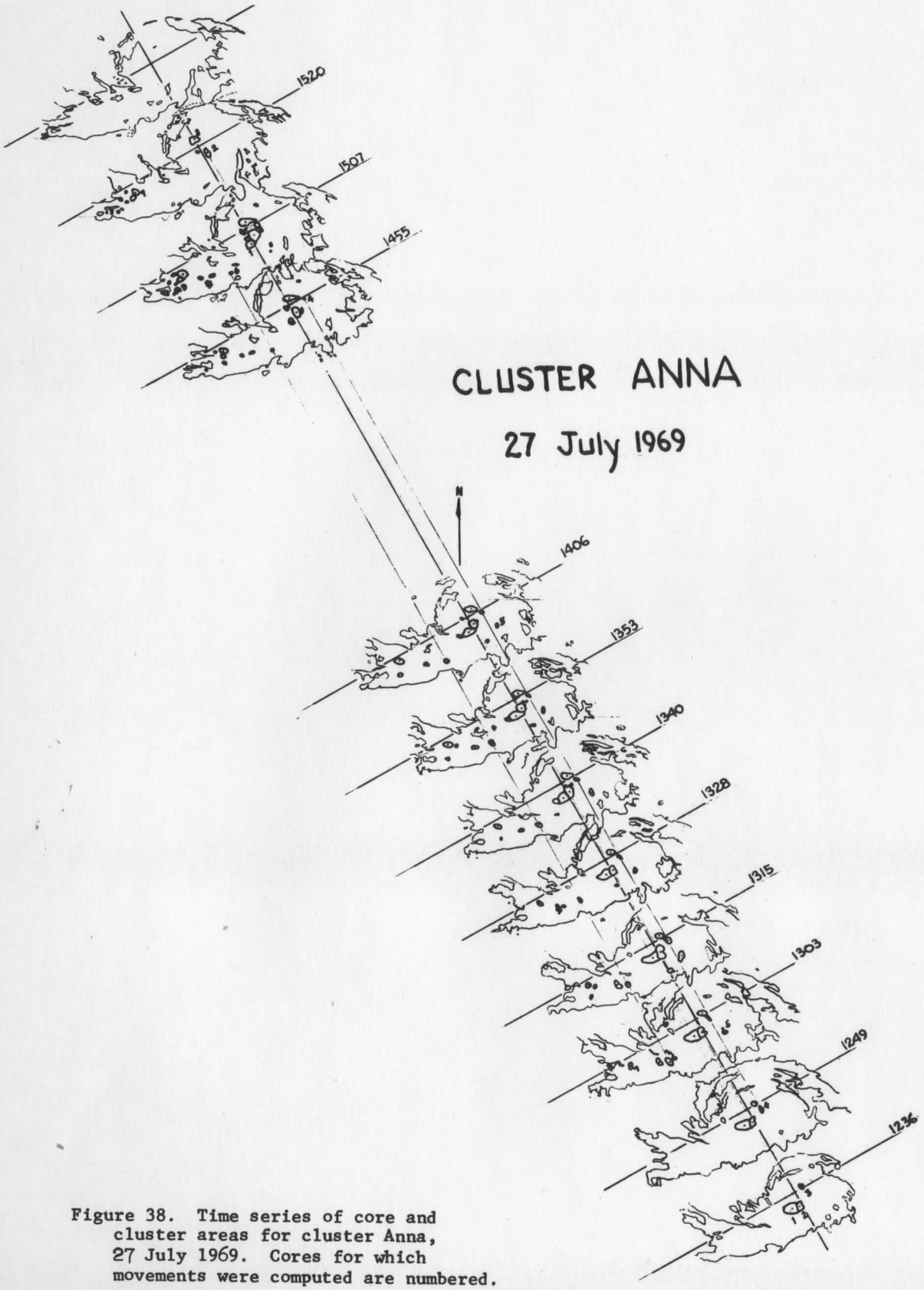

Figure 38. Time series of core and cluster areas for cluster Anna, 27 July 1969. Cores for which movements were computed are numbered.

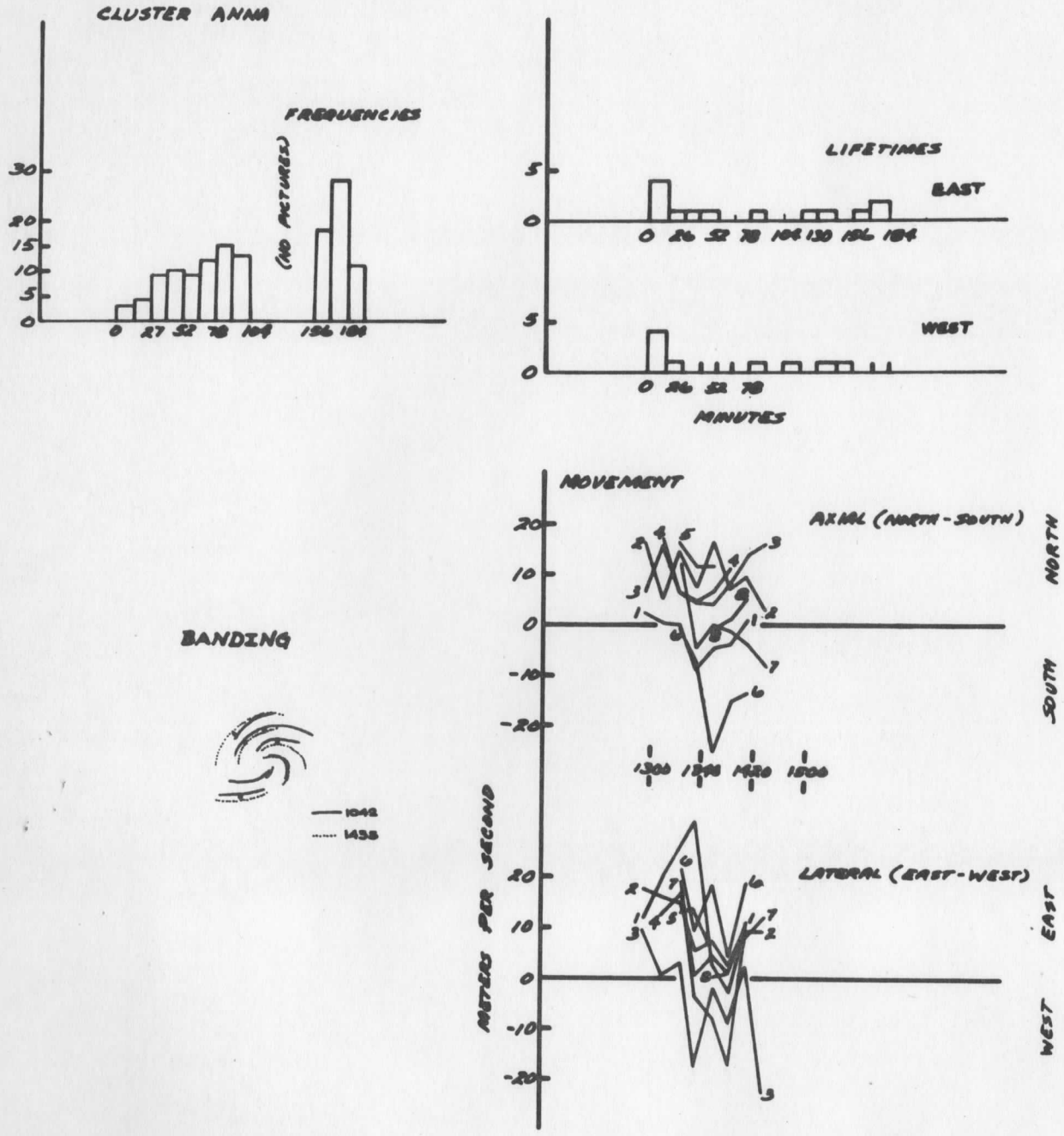

Figure 39. Core characteristics for cluster Anna, 27 July 1969.

had a wide distribution of sizes. There was a mild tendency toward ellipticity, with long axes of cores conforming to the spiral lines of the vortex.

In the determination of the lifetime distribution no new cores were considered after 1406Z. Making allowance for three missing pictures between 1406 and 1455, lifetimes were generally under an hour or 1.5 to 3 or more hours. Classification of lifetimes by vortex and tail groups shows the vortex group having 20% longer average lifetimes.

The most remarkable feature of this cluster was the rotation of cores in the eastern group around an "eye" which was the reference point for the series. This rotation was measured to be about 1.7 revolutions per day. Since the distance between core centers across the eye was roughly 110 km, core rotational velocity was close to 13 m/sec. This corresponds to a relative vorticity of 2×10^{-4} sec^{-1}. Cores in the tail moved eastward relative to the eye at speeds which diminished from 30 m/sec (core closest to the vortex) to 7 m/sec (long lived core at the western end). Evidently the cyclonic circulation of this storm extended through a deep layer of the atmosphere. The extent of its horizontal influence is shown in cyclonic banding of low cloud out to 800 km east, north, and west of the eye.

IV. Summary and Conclusions

It has been shown that (1) signal enhancement is an effective, precise tool for isolating selected features of ATS images; (2) very bright regions of the ATS image correlate well with large radar echoes; (3) properly enhanced ATS pictures isolate areas of deep convection; (4) deep convection can be studied over a three or four hour period around local noon on unnormalized pictures; and (5) a simple cosine law normalization can appreciably extend this period.

The use of enhancement with conventional cloud census techniques shows the eastern Atlantic to be at least as convectively active as the western Atlantic during June and July, and to have a significantly greater total area of cloud clusters.

Studies of convective cores reveal a great range of size, spacing, and lifetime; nevertheless an ordering invariably can be perceived. This most often is as lines or bands; waves, spirals, and solitary cores are also observed. Lifetimes are a few minutes to several hours or more; large cores last longer.

Displacement of cloud clusters is accomplished by a complex combination of band and cell movement and propagation. Structure, as evidenced by core behavior, is varied and complex.

It is recommended as a result of this investigation that:

- every data channel on future meteorological satellites should be equipped with a calibration signal added to the data signal at the sensor or as close to the sensor as is possible. This calibration must be retained through the archive stage of data processing.

- adjustments to data signals from existing meteorological satellites should be limited and strictly controlled. All changes should be documented, and the complete documentation of signal levels should accompany the data.
- comparisons of ATS and radar images should be extended. The integration of sophisticated forms of ATS - e.g. enhanced, normalized pictures, digital mappings, and cloud tracers - and concentrations of conventional data from, for example, the Line Islands Experiment or BOMEX, is a highly productive way to further understanding of cloud clusters.

REFERENCES

BOMEX Bulletin No. 3, Jan. 27, 1969.

Frank, N. L., 1970: "Atlantic Tropical Systems of 1969," Month. Weather Rev., 98: 4, 307-314.

Gage, Richard, 1971: personal communication.

Hudlow, M. D., Sept. 1970: "Weather Radar Investigations on the BOMEX," Research and Devt. Technical Report ECOM-3329.

Martin, D. W., and O. Karst, 1969: "A Census of Cloud Systems Over the Tropical Pacific," Studies in Atmospheric Energetics Based on Aerospace Probings - Annual Report - 1968, Space Science and Engineering Center, Univ. of Wisconsin.

Parent, R. J., 1971: Preliminary Report - ATS - III Data System Error Analysis (Wind Determination Only), Univ. of Wisconsin.

Phillips, Dennis R., 1971: personal communication.

Plan for U. S. Participation in the GARP Atlantic Tropical Experiment, 1971: Report of the ad-hoc Tropical Task Group to the U. S. Committee for GARP Nat. Research Council, NAS, Washington, D. C.

The Planning of GARP Tropical Experiments, Jan. 1970: GARP Publication Series No. 4.

Report of the Fifth Session of the JOC, Bombay, 1-5 February, 1971.

Report of the Informal Planning Meeting on the Use of Aircraft in GATE, Geneva, 10-14 May 1971.

Report of Planning Conference on GARP - Brussels, March 1970: GARP Special Report No. 1.

Ruff, I., R. Koffler, S. Fritz, J. S. Winston, and P. K. Rao, 1967: "Angular Distribution of Solar Radiation Reflected from Clouds as Determined by TIROS IV Radiometer Measurements," ESSA Technical Report NESC-38, U. S. Dept. of Commerce, Washington, D. C.

Schwalenberg, Terry W., 1971: The ATS Video Enhancer, Space Science and Engineering Center, Univ. of Wisconsin.

Simpson, R. H., and J. M. Pelissier, 1971: "Atlantic Hurricane Season of 1970," Month. Weather Rev., 99: 4, 269-277.

Simpson, R. H., A. L. Sugg, and Staff, 1970: "The Atlantic Hurricane Season of 1969," Month. Weather Rev., 98: 4, 293-306.

Smith, E., 1971: Reference Manual for ATSLIB (1108 Program File), Space Science and Engineering Center, Univ. of Wisconsin.

Taylor, V. R., 1970: "Operational Brightness Normalization of ATS - I Cloud Pictures," ESSA Technical Memo NESCTM 24, U. S. Dept. of Commerce, Washington, D. C.

Technical Data Report for ATS, 1968: Goddard Space Flight Center, Greenbelt, Md.

Vonder Haar, T. H., and R. S. Cram, 30 Sept. 1970; A Pilot Study on the Application of Geosynchronous Meteorological Satellite Data to Very Short Range Terminal Forecasting, Space Science and Engineering Center, Univ. of Wisconsin.